© 2015. Published by The Company of Biologists Ltd | Development (2015) 142, 994-1005 doi:10.1242/dev.115352

RESEARCH ARTICLE

Drosophila small heat shock protein CryAB ensures structural integrity of developing muscles, and proper muscle and heart performance

Inga Wójtowicz[1,2], Jadwiga Jabłońska[2], Monika Zmojdzian[1], Ouarda Taghli-Lamallem[1], Yoan Renaud[1], Guillaume Junion[1], Malgorzata Daczewska[2], Sven Huelsmann[3], Krzysztof Jagla[1] and Teresa Jagla[1,*]

ABSTRACT

Molecular chaperones, such as the small heat shock proteins (sHsps), maintain normal cellular function by controlling protein homeostasis in stress conditions. However, sHsps are not only activated in response to environmental insults, but also exert developmental and tissue-specific functions that are much less known. Here, we show that during normal development the *Drosophila* sHsp CryAB [L(2)efl] is specifically expressed in larval body wall muscles and accumulates at the level of Z-bands and around myonuclei. CryAB features a conserved actin-binding domain and, when attenuated, leads to clustering of myonuclei and an altered pattern of sarcomeric actin and the Z-band-associated actin crosslinker Cheerio (filamin). Our data suggest that CryAB and Cheerio form a complex essential for muscle integrity: CryAB colocalizes with Cheerio and, as revealed by mass spectrometry and co-immunoprecipitation experiments, binds to Cheerio, and the muscle-specific attenuation of *cheerio* leads to *CryAB*-like sarcomeric phenotypes. Furthermore, muscle-targeted expression of CryAB^{R120G}, which carries a mutation associated with desmin-related myopathy (DRM), results in an altered sarcomeric actin pattern, in affected myofibrillar integrity and in Z-band breaks, leading to reduced muscle performance and to marked cardiac arrhythmia. Taken together, we demonstrate that CryAB ensures myofibrillar integrity in *Drosophila* muscles during development and propose that it does so by interacting with the actin crosslinker Cheerio. The evidence that a DRM-causing mutation affects CryAB muscle function and leads to DRM-like phenotypes in the fly reveals a conserved stress-independent role of CryAB in maintaining muscle cell cytoarchitecture.

KEY WORDS: *Drosophila*, Cheerio, CryAB, Heart, Muscle, sHsp

INTRODUCTION

Most heat shock proteins operate as molecular chaperones in stress conditions and play a central role in the maintenance of normal cellular function by preventing the aggregation of misfolded proteins into large deleterious complexes (Morimoto, 1998). However, some heat shock proteins are also activated in a stress-independent way to control the transport, folding, assembly and degradation of various proteins (Colinet et al., 2010; Lindquist and Craig, 1988; Mymrikov et al., 2010; Sorensen et al., 2003). The cell-specific expression of small heat shock proteins (sHsps) during development, cell differentiation or after activation by growth factors and oncogenes has been reported in a wide range of organisms, including *Drosophila* and mammals (Michaud and Tanguay, 2003; Morimoto, 1998). For example, the *Drosophila* sHsp Hsp22, in spite of its heat-induced expression and nonspecific chaperone activity, is regulated during normal development and plays a role in protection against apoptosis (Colinet et al., 2010; Morrow and Tanguay, 2003).

In human, seven sHsps are expressed in cardiac and skeletal muscles, including αB-crystallin (*CRYAB*), *HSPB2* and *HSPB3*; they are induced during the initial phase of skeletal muscle differentiation, controlled by MYOD1, suggesting a muscle-specific function in development. Also, Hspb2 and CryAB proteins display sarcomeric localizations; they are localized on Z-bands or I-bands of the skeletal and cardiac muscle myofibrils, maintaining and protecting contractile cytoskeletal structures (Mymrikov et al., 2010; Sugiyama, 2000).

CryAB displays particularly intriguing cell-specific functions, acting as a chaperone for intermediate filament (IF) proteins such as desmin in muscle cells and vimentin in eye lenses. IFs are known to overlie Z-discs and M-lines, stabilizing myofibrils and protecting them from mechanical insult (Goldfarb and Dalakas, 2009). IFs also link membranous organelles, such as nuclei and mitochondria, and play an important role in maintaining their correct morphology and positioning.

CryAB stabilizes IFs and prevents them from aggregating under stress conditions, and also assists IFs during developmental reorganizations (Nicholl and Quinlan, 1994). Importantly, mutations in CryAB, such as replacement of arginine by glycine at conserved position 120 (R120G), lead to altered CryAB-IF interactions responsible for desmin-related myofibrillar myopathy (DRM) (Dalakas et al., 2000; Goldfarb and Dalakas, 2009; Goldfarb et al., 2004). The R120G missense mutation alters the spatial organization of CryAB, leading to the loss of its chaperone activity and the formation of desmin aggregates in muscle fibers (Vicart et al., 1998; Perng et al., 2004). As a result, the desmin IF network is severely affected, leading to altered myofibril alignment, irregular sarcomere architecture and abnormal mitochondrial organization (Goldfarb and Dalakas, 2009). In DRM patients this leads to progressive muscle weakness, including the limb, neck and respiratory muscles, for which no appropriate treatments have yet been developed.

To further characterize muscle-specific roles of CryAB and better understand DRM-associated muscle defects we took advantage of its evolutionary conservation to analyze the function of the *Drosophila* CryAB counterpart. The fruit fly *Cryab* ortholog, *CryAB*, which is also known as *lethal (2) essential for life* [*l(2)efl*], has been shown to

[1]GReD - INSERM U1103, CNRS UMR6293, Clermont Université, 28, place Henri Dunant, Clermont-Ferrand 63000, France. [2]Department of Animal Developmental Biology, Institute of Experimental Biology, University of Wrocław, Sienkiewicza 21, Wrocław 50-335, Poland. [3]Wellcome Trust/Cancer Research UK Gurdon Institute and Department of Physiology, Development and Neuroscience, University of Cambridge, Tennis Court Road, Cambridge CB2 1QN, UK.

*Author for correspondence (teresa.jagla@udamail.fr)

Received 12 July 2014; Accepted 15 January 2015

Development (2015) 142, 994-1005 doi:10.1242/dev.115352

be involved in the modulation of insulin signaling and the regulation of lifespan (Flatt et al., 2008) but its expression and function in differentiated muscle have not been analyzed.

Here we show that, like its vertebrate counterpart, the *Drosophila* CryAB protein displays stress-independent muscle-specific expression. In larval muscles it accumulates around the myonuclei and at the level of Z-bands and is required for correct nuclei localization, myofibril integrity and muscle performance. CryAB features a conserved actin-binding domain and is required for the correct sarcomeric pattern of actin filaments and also of the Z-band-associated actin crosslinker Cheerio. CryAB binds to Cheerio in muscles, indicating that this interaction might help to maintain myofibrillar integrity in *Drosophila* muscle. We also report that muscle-targeted expression of CryAB carrying the DRM-associated R120G mutation leads to severe alterations in the striated actin pattern, reduced muscle performance and marked cardiac arrhythmia. These observations point to a conserved stress-independent role of CryAB in the maintenance of muscle cell cytoarchitecture. Thus, our findings provide evidence that the *Drosophila* sHsp CryAB shares not only sequence but also functional similarities with its human counterpart, suggesting that *Drosophila* can serve as a model system for dissecting molecular determinants of myofibrillar myopathies.

RESULTS

Drosophila CryAB is a conserved sHsp with stress-independent expression in larval body wall muscles

The *Drosophila* sHsp genes are clustered within the 67B region on the left arm of the third chromosome (Corces et al., 1980), except for *CryAB* [l(2)efl], which is located on the right arm of the second chromosome (Kurzik-Dumke and Lohmann, 1995). *Drosophila* CryAB shows significant homology to human CRYAB (Fig. 1A) and to other sHsp members, in particular the Hspb1 and Hspb8 subfamilies (Fink et al., 2009; McWilliam et al., 2013) (Fig. 1C). *CryAB* encodes a protein of ~22 kDa (Fig. 1B) that has a highly conserved α-crystallin domain located in the C-terminal portion of the protein (Fig. 1A), similar to other sHsps (Ingolia and Craig, 1982). Within this domain, CryAB features several conserved motifs, including an actin-binding domain, a capping box and the residues R120 and D109 involved in desminopathies (Fig. 1A).

In addition to coordinately induced expression in response to a heat stress, several members of the sHsp family show a specific pattern of expression in diverse tissues and cells (Marin and Tanguay, 1996; Michaud and Tanguay, 2003). To determine whether *CryAB* also displays stress-independent expression during development we first analyzed its expression pattern in third instar larvae. Using a polyclonal antibody raised against the whole CryAB protein, we found that CryAB is abundantly expressed in the larval body wall muscles (Fig. 2). Within an individual larval muscle, CryAB accumulated in the perinuclear area (Fig. 2A) and displayed a striated sarcomeric pattern at the level of Z-lines and M-lines (Fig. 2A-D). We confirmed this observation by the immunogold detection of CryAB on the ultrathin sections visualized in electron microscopy (EM) (supplementary material Fig. S1). When analyzing CryAB distribution on longitudinal optical sections through the muscle fibers, we also found that it accumulated around the nuclei and enveloped the external surface of myonuclei (Fig. 2E). We observed a granular pattern of CryAB both around

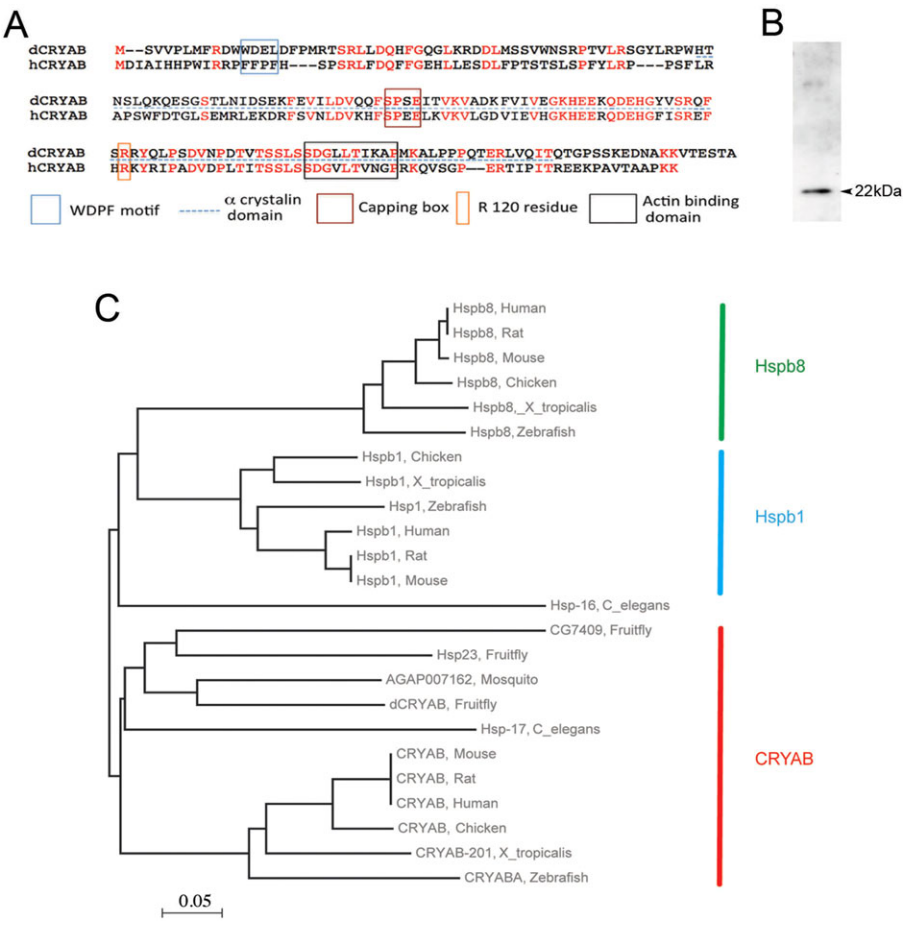

Fig. 1. *Drosophila* CryAB is a highly conserved member of the CryAB sHsp family that is phylogenetically related to the Hspb1 and Hspb8 sHsp families. (A) Protein sequence alignment of *Drosophila* and human CryAB proteins. Conserved amino acid residues are in red and conserved functional domains are highlighted by boxes or underlining. (B) Western blot of third instar larvae protein extract showing the 22 kDa band of the expected size of CryAB protein. (C) Phylogenetic tree of the related CryAB, Hspb1 and Hspb8 families.

Development (2015) 142, 994-1005 doi:10.1242/dev.115352

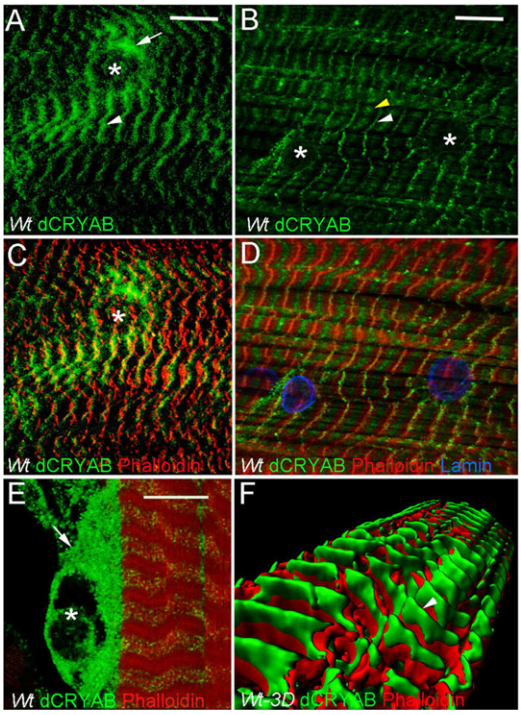

Fig. 2. CryAB displays Z-band-associated and perinuclear expression in larval muscles. (A,C) CryAB expression at the superficial level of external myofibrils. Note the accumulation of CryAB at the level of Z-bands (arrowhead) and around the nuclei (arrow). (B,D) CryAB expression within the myofiber. CryAB protein is detected at the Z-bands (white arrowhead) but also in M-lines (yellow arrowhead). (E) A portion of larval segment border muscle at the level of the nuclei. Note high CryAB accumulation in a perinuclear area (arrow) and at the external surface of the nucleus. (F) Imaris-rendered 3D reconstruction of confocal scans through ventral VL3 larval muscle stained for CryAB and with phalloidin (F-actin). Note the external localization of CryAB on the top of phalloidin-stained Z-bands (arrowhead). Asterisks indicate nuclei. Scale bars: 10 µm.

the nuclei (Fig. 2E) and at the Z-discs (Fig. 2B,D), indicating that it might be part of large protein complexes. 3D reconstruction of confocal scans (Fig. 2F) revealed that the Z-line-associated CryAB is mainly localized at the external level of Z-discs. This developmental expression pattern of *Drosophila* CryAB is reminiscent of that of its human ortholog (Dubin et al., 1990).

CryAB is required for Z-band patterning and muscle integrity

To assess the role of *CryAB* in larval muscles we applied RNAi-mediated muscle-specific gene attenuation (Fig. 3I) using two different *UAS-CryAB-RNAi* lines (VDRC 40532 and 107305) crossed to the *Mef2-Gal4* driver (Fig. 3; supplementary material Fig. S2). We observed that most *Mef2>CryAB-RNAi* larvae (from both RNAi lines examined) exhibited defects in sarcomeric organization, characterized by an irregular, fuzzy pattern of phalloidin staining in the large muscle segments (Fig. 3C,H; supplementary material Fig. S2). This aberrant organization of sarcomeric actin is consistent with the fact that CryAB has an actin-binding domain (ABD) (see Fig. 1), which appears to play an important role in actin filament organization assuming that muscle-targeted expression of CryAB carrying a mutated ABD leads to RNAi-like phenotypes (supplementary material Fig. S3). Moreover, *CryAB* attenuation also leads to muscle splitting (Fig. 3B; supplementary material Fig. S4A), which in some cases is associated with altered muscle attachments (Fig. 3B) or even with

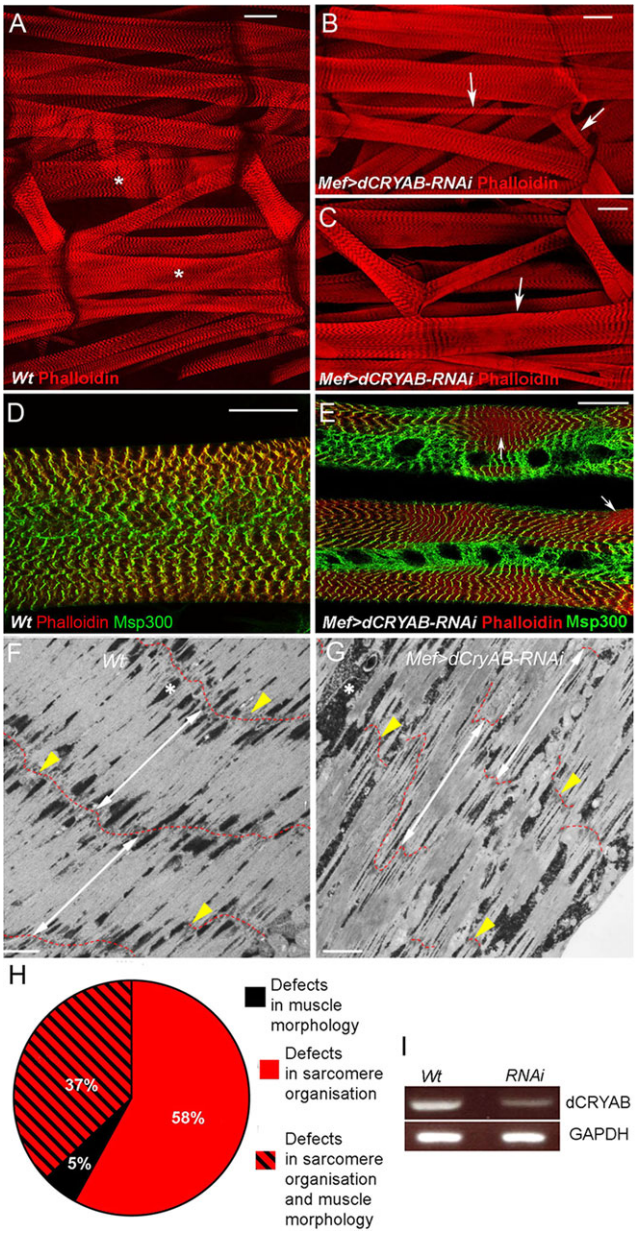

Fig. 3. Muscle-specific attenuation of *CryAB* leads to morphological muscle defects and disrupted sarcomeric Z-band pattern. (A) Lateral view of wild-type third instar larval muscles stained with phalloidin. (B,C) Effects of muscle-targeted RNAi attenuation of *CryAB*. Arrows in B indicate splitting of myofibers. Arrow in C denotes fuzzy Z-band pattern; compare with wild-type muscles (asterisks in A). (D) A portion of wild-type VL3 muscle showing a regular pattern of Msp300 co-stained with phalloidin. (E) Representative view of a portion of VL3 and VL4 muscles from *Mef2>CryAB-RNAi* animals. Arrows point to muscle areas with a fuzzy actin pattern in which Msp300 labeling is reduced or missing. (F) EM view of wild-type VL4 sarcomeres. (G) Similar view from *Mef2>CryAB-RNAi* larvae showing interrupted Z-bands. Yellow arrowheads point to Z-bands, which are also traced by the red line. Asterisks indicate electron-dense accumulations of glycogen. Double-ended arrows indicate the extension of sarcomeres. (H) Statistical representation of muscle defects observed in *Mef2>CryAB-RNAi* larvae. (I) RT-PCR analysis of *CryAB* attenuation in *Mef2>CryAB-RNAi* versus wild-type (Wt) larvae. *Gapdh* provides a loading control. Scale bars: 20 µm in A-E; 2 µm in F,G.

the loss of affected muscle (supplementary material Fig. S4B). The observed muscle defects are not due to apoptotic events, as we do not detect Caspase 3 activation associated with muscles in the *CryAB-RNAi* context (supplementary material Fig. S2I). Altogether, these

Development (2015) 142, 994-1005 doi:10.1242/dev.115352

findings demonstrate a role of CryAB in the maintenance of muscle fiber integrity.

To better characterize the influence of *CryAB* attenuation on the sarcomeric pattern we used Msp300 antibody to reveal the Z-bands (Fig. 3D,E). We found that, in the muscle segments displaying fuzzy phalloidin staining, the Z-band-associated signal of Msp300 was weak or lacking (Fig. 3E). We also noted that Msp300 was irregularly distributed around the myonuclei (Fig. 3D,E), suggesting that it might potentially interact with CryAB. We tested this possibility by co-immunoprecipitation (co-IP) (supplementary material Fig. S5) and found that there is no physical interaction between these two Z-disk-associated proteins. Gaps in Z-bands were also detected when examining EM sections of *CryAB* attenuated muscles (Fig. 3F,G), supporting the view that CryAB acts to stabilize Z-band-associated sarcomeric components.

Assuming that each of the larval muscles displays a specific number of sarcomeres (Bate, 1990), we also tested whether muscle-targeted *CryAB* knockdown impacted on sarcomere number. We focused on three distinct muscles (VL3, VL4 and SBM) and found that, in all cases, the number of sarcomeres was significantly reduced (supplementary material Fig. S4A), whereas, except for the fuzzy pattern areas, the size of sarcomeres was unaffected (supplementary material Fig. S4B). Thus, CryAB also appears to play a role in larval muscle growth, which occurs by the addition of sarcomere units.

CryAB is required for correct myonuclei localization, mitochondrial organization and muscle performance

Next we investigated whether the cellular organization and the performance of muscles are affected by the reduction of CryAB function. Previous studies demonstrated that the localization of nuclei is crucial for proper muscle performance (Metzger et al., 2012) and that mitochondria are highly organized in muscles (Picard et al., 2012). The accumulation of CryAB around the nuclei (Fig. 2) prompted us to test whether it was involved in the correct distribution of myonuclei within the muscle fibers. We found that in the *CryAB-RNAi* context they were irregularly distributed along the muscle fibers (Fig. 4A,B). Nuclei are also misarranged in muscles overexpressing CryAB with a mutated ABD (supplementary material Fig. S3), providing evidence that the actin binding function of CryAB is essential for nuclei localization.

Cheerio, which makes a link between perinuclear actin and cytoplasmic actin cables, is involved in nuclei positioning in *Drosophila* nurse cells (Huelsmann et al., 2013). It is also well known that in vertebrate muscles the Cheerio ortholog Filamin C is associated with Z-bands and when mutated leads to myofibrilar myopathies (Goldfarb and Dalakas, 2009). We tested whether Cheerio is expressed in larval muscles and whether CryAB influences its localization. Cheerio was detected aligned with Z-bands (Fig. 4C), but its pattern was more expansive than the sharp Z-line revealed by phalloidin. As in nurse cells, it also accumulated in the perinuclear area. However, in muscles attenuated for *CryAB* the sarcomeric localization of Cheerio was severely affected, with pronounced accumulation around the mislocalized nuclei (Fig. 4D), strongly suggesting that CryAB is required for Cheerio localization. In addition, the mitochondrial signal appeared significantly reduced in *CryAB-RNAi* muscles compared with the wild type (Fig. 4E,F), indicating impaired respiratory functions. This possibility was supported by EM analysis revealing mitochondrial swelling, broken cristae and glycogen deposits (Fig 4G,H).

To test whether the described morphological alterations affected the locomotive abilities of larvae, we carried out three behavioral tests. We measured the speed of crawling and found that

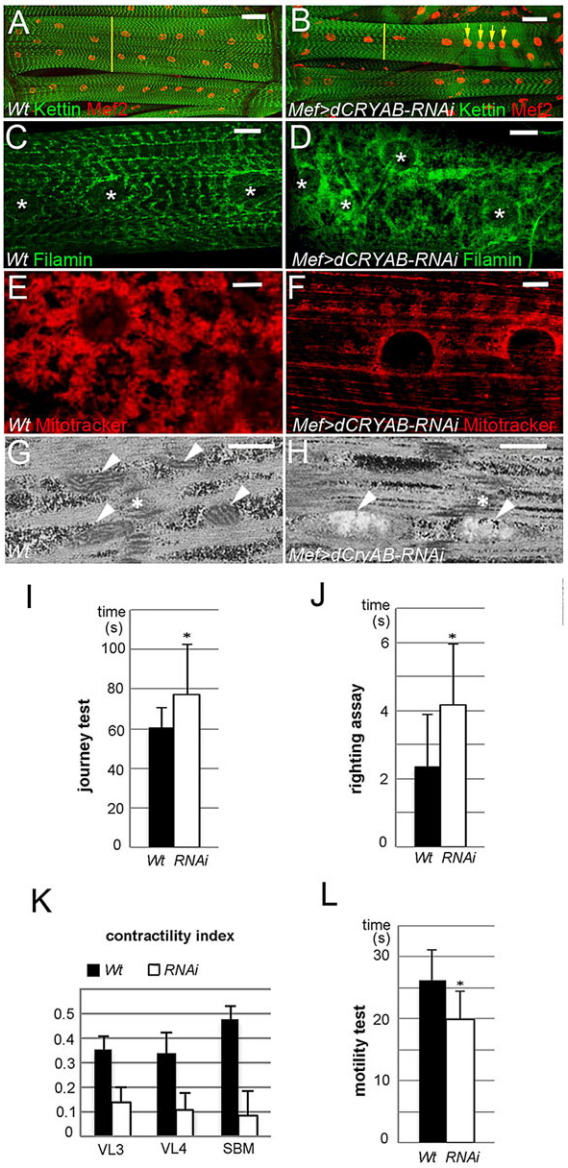

Fig. 4. CryAB is required for muscle integrity and performance. (A) Distribution of nuclei in wild-type VL3 and VL4 muscles. VL3 muscle diameter is indicated by the yellow line. A slightly reduced number of nuclei is observed in muscles with attenuated *CryAB*, which could be due to destabilization of myofibrillar architecture and subsequent loss of some of mislocalized nuclei. (B) *Mef2>CryAB-RNAi* VL3 muscles displayed reduced diameter (yellow line) and mislocalized nuclei (arrows). (C) Wild-type pattern of Z-band-associated Cheerio. Asterisks indicate nuclei. (D) Disrupted Cheerio pattern in *Mef2>CryAB-RNAi* context. (E) Wild-type pattern of mitochondria revealed by MitoTracker Red. (F) Attenuation of *CryAB* leads to a reduced MitoTracker signal. (G) EM view of wild-type third instar muscle with functional mitochondria. (H) EM view of a *Mef2>CryAB-RNAi* muscle with morphologically abnormal mitochondria. Arrowheads indicate mitochondria and asterisks indicate the Z-band. (I-L) Muscle performance tests showing reduced motility and affected contractility of *Mef2>CryAB-RNAi* larvae. Error bars indicate s.e.m.; n=30 flies per genotype *P<0.05 (one-way ANOVA). Scale bars: 20 µm in A,B; 10 µm in C,D; 5 µm in E,F; 1 µm in G,H.

CryAB-RNAi larvae needed ~20% more time to travel the appointed distance (Fig. 4I). We also measured the time needed for each larva to right itself from the dorsal to ventral position. In this test, *CryAB*-attenuated individuals took twice as long (Fig. 4J). Finally, the number of peristaltic movements of crawling larvae was counted: during a 30 s period, *CryAB-RNAi* specimens executed at

Development (2015) 142, 994-1005 doi:10.1242/dev.115352

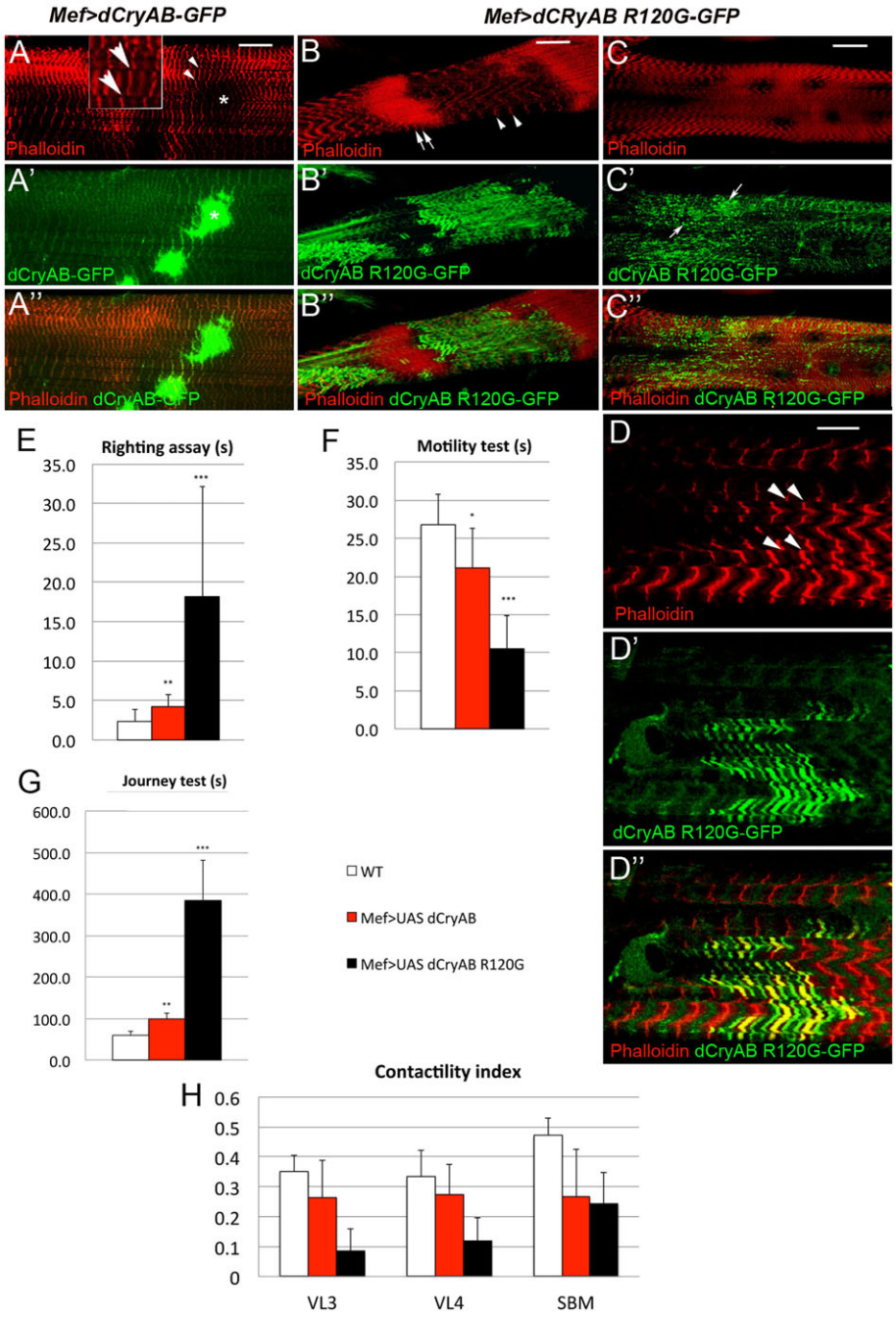

Fig. 5. Defective structural integrity and muscle performance induced by muscle-targeted expression of CryAB^{R120G}. (A-A″) Z-band pattern in the muscle area with accumulation of wild-type CryAB-GFP. Note the Z-line shift (arrowheads, magnified in inset) close to the spot of CryAB-GFP accumulation. (B-B″) Irregular phalloidin staining in muscle expressing CryAB^{R120G}-GFP. Note that muscle portions with high levels of CryAB^{R120G}-GFP display a weak phalloidin signal with an increased distance between Z-bands (arrowheads), whereas the areas devoid of CryAB^{R120G}-GFP show a condensed sarcomeric pattern (arrows) with high phalloidin signal. (C-C″) Muscle portion with targeted expression of CryAB^{R120G}-GFP showing aggregate-like pattern of GFP (arrows). (D-D″) A detailed view of sarcomeric localization of CryAB^{R120G}-GFP expressed under the *Mef2-Gal4* driver. Note that CryAB^{R120G} is detected in Z-lines and also in two bands on each side of the Z-disk. Arrowhead indicates Z-line shift that coincides with the accumulation of CryAB^{R120G}-GFP. (E-H) Muscle performance tests showing reduced motility and affected contractility of *Mef2>CryAB^{R120G}-GFP* larvae. Error bars indicate s.e.m.; n=28 flies per genotype; *P<0.05, **P<0.005, ***P<0.0005 (one-way ANOVA). Scale bars: 30 µm in A,B; 20 µm in C; 10 µm in D.

least 20% fewer peristaltic movements than controls (Fig. 4L). To confirm the contraction disturbance, we also compared the length of muscle fibers relaxed by EDTA with that of contracted muscle fibers. This showed that the analyzed muscles from *CryAB-RNAi* individuals had a significantly lower contractility index (Fig. 4K). Thus, these data show that CryAB is required for proper muscle contraction and efficient motility. Finally, we found that these functions of CryAB in muscles also influence the survival of flies (supplementary material Fig. S3C).

The R120G mutation of DRM patients leads to a dominant-negative CryAB protein and affects sarcomeric pattern and muscle performance

DRM is caused by the missense R120G mutation within the α-crystallin domain of CRYAB. It is due to intracellular aggregations of desmin and Vimentin IFs, which abnormally interact with the mutated CRYAB (Simon et al., 2007; Zobel et al., 2003). Comparison of amino acid sequences of human and *Drosophila* CryAB proteins showed conservation of arginine at position 120 (Fig. 1A) and prompted us to test whether the R120G mutation in *Drosophila* CryAB could mimic muscle defects observed in DRM patients. We generated transgenic lines carrying either the wild-type or mutated form of CryAB fused to GFP (Fig. 5A-D″).

Compared with endogenous CryAB (Fig. 2), both CryAB-GFP and CryAB^{R120G}-GFP displayed irregular accumulations along the muscle fibers in addition to their localization in sarcomeres (Fig. 5A′-D′). We therefore tested whether these accumulations affected sarcomeric organization. In the area where the wild-type CryAB-GFP accumulated, the sarcomeric pattern marked with phalloidin

Development (2015) 142, 994-1005 doi:10.1242/dev.115352

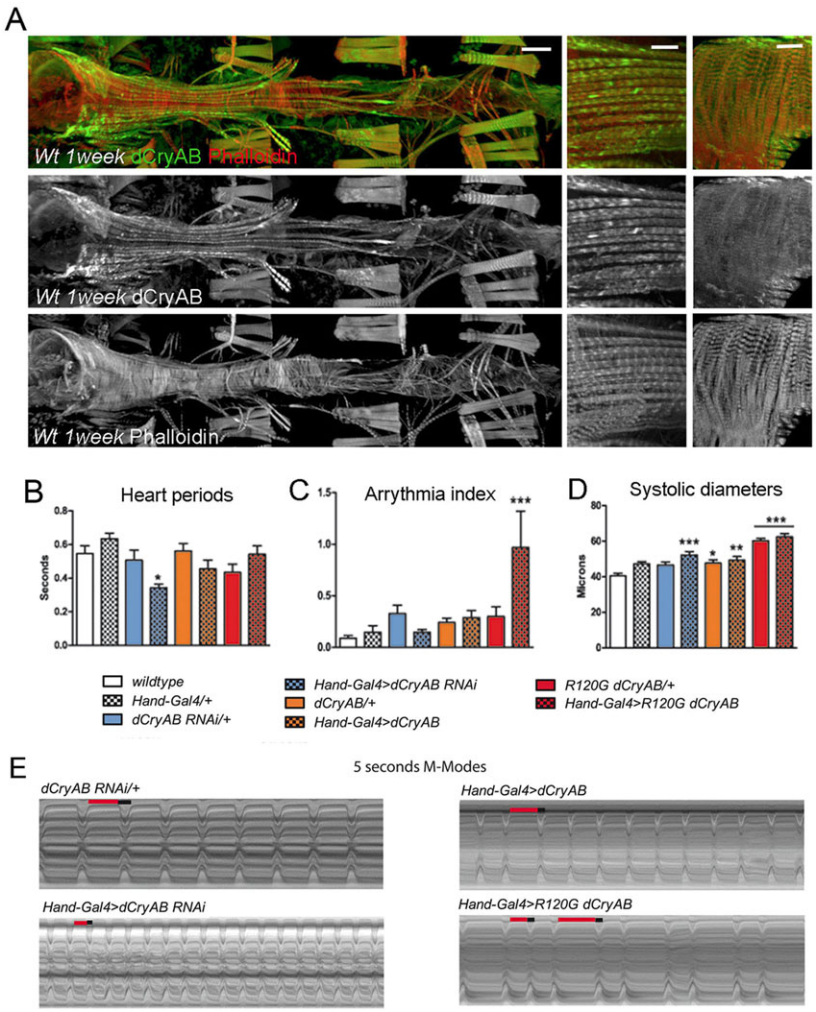

Fig. 6. Cardiac-specific attenuation of *CryAB* and expression of *CryAB*^{R120G} affect heart performance. (A) Dorsal view of dissected adult heart from a 1-week-old fly stained for CryAB and with phalloidin (left panels show an overview). CryAB is expressed in longitudinal fibers associated with the heart (middle panels) and the transverse myofibrils of the cardiac muscle (right panels). (B-D) Heart period (B), arrhythmia index (C) and systolic diameter (D) of 1-week-old flies of the indicated genotypes. Note that knockdown of *CryAB* shows significant shortening in the heart periods (B). Upon expression of *CryAB*^{R120G}, the arrhythmia index is substantially increased (C) and systolic diameter is enlarged (D). Error bars indicate s.e.m.; *N*=20 flies per genotype and age. **P*<0.05, ***P*<0.005, ****P*<0.0005 (one-way ANOVA). (E) Representative M-mode traces (5 s) illustrating movements of heart tube walls (*y*-axis) over time (*x*-axis). Movement traces of cardiac tubes expressing *CryAB-RNAi* illustrate the increased heart rate and the rhythmic beating patterns. M-modes from hearts expressing *CryAB*^{R120G} reveal arrhythmic beating patterns. Diastolic (red) and systolic (black) intervals are indicated in each M-mode trace. Scale bars: 200 µm in A, left; 25 µm in A, middle and right.

appeared normal, although the intensity of actin bands was attenuated (Fig. 5A-A″, asterisk). Occasionally, we observed misalignments of myofibrils (Fig. 5A, arrowheads), suggesting that the overexpression of CryAB leads to a local destabilization of myofibrillar organization. In contrast to these mild phenotypes, the accumulations of CryAB^{R120G} resulted in severely altered sarcomeric patterns (Fig. 5B-D″), with virtually all muscles affected. We observed a striking complementary distribution of CryAB^{R120G} with respect to sarcomeric actin along the muscles. Large segments of muscle fibers with high levels of CryAB^{R120G} displayed reduced phalloidin staining with abnormally interspaced and irregular Z-bands (Fig. 5B, arrowheads), whereas the neighboring CryAB^{R120G}-free regions were characterized by a high-intensity phalloidin signal probably resulting from the disorganization and local compaction of sarcomeres (Fig. 5B, arrows). In addition to localizing to the Z-bands, CryAB^{R120G} accumulated in either a fuzzy pattern (Fig. 5B′,B″) or a punctate pattern suggesting the formation of aggregates (Fig. 5C′,C″). We also observed small patches of accumulated CryAB^{R120G} (Fig. 5D-D″) in which the sarcomeric pattern was not particularly affected. However, we noted that within each sarcomere CryAB^{R120G} was not only present in the Z-bands but also in two additional stripes between the Z-bands (Fig. 5D″), and that myofibrils were misaligned (Fig. 5D, arrowheads).

These alterations prompted us to test whether the mutated form of CryAB also affected larval muscle function. We tested muscle performance using the righting, motility and journey tests. In all these tests (Fig. 5E-G), *Mef2>CryAB*^{R120G} larvae showed markedly reduced muscle performance than those expressing wild-type CryAB in muscles. We also found that muscle-targeted expression of CryAB^{R120G} affected muscle contractility (Fig. 5H). The fact that several phenotypes of CryAB^{R120G} overexpression are similar to those observed after knocking down *CryAB* suggests that CryAB^{R120G} acts as a dominant negative.

Cardiac-specific attenuation of *CryAB* and expression of *CryAB*^{R120G} impair heart performance

A recent study demonstrated that when the mutated human *CRYAB* is expressed in adult *Drosophila* heart it mimics DRM-related cardiac defects such as arrhythmia and an increase in systolic heart diameter (Xie et al., 2013). However, it remained unclear whether these defects were due to reduced functions of the endogenous *Drosophila CryAB* gene. We therefore tested whether CryAB is expressed in the adult *Drosophila* heart and if it is required for normal heart function.

We found that CryAB protein is present in a striated pattern in both the transverse myofibrils of the myocardium and in the layer of the longitudinal muscle fibers that is associated with the heart (Fig. 6A). This CryAB expression plays an important role in the adult heart because the heart-specific attenuation of *CryAB* resulted in an accelerated cardiac rhythm (Fig. 6B,E). The video-captured M-modes of hearts revealed a reduction in the heart period following RNAi-mediated *CryAB* knockdown, as compared with

Development (2015) 142, 994-1005 doi:10.1242/dev.115352

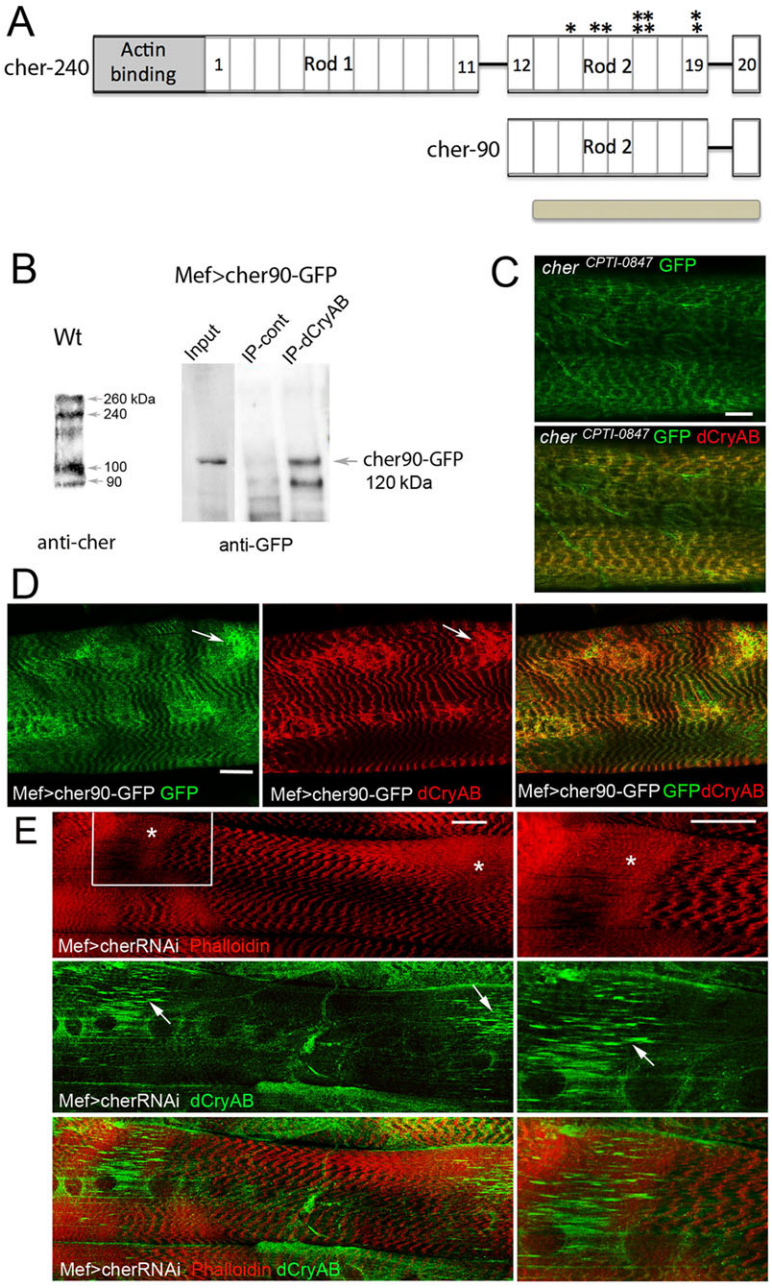

Fig. 7. CryAB interacts with Cheerio. (A) Schematic representation of the cher-240 and cher-90 isoforms. Asterisks indicate the location of peptides identified by mass spectrometry. The bar beneath indicate the region recognized by anti-Cheerio antibody. (B) (Left) Western blot showing the different Cheerio isoforms detected in protein extract from third instar larvae. (Right) Western blot from IP with anti-CryAB antibody on protein extract from third instar *Mef2>cher-90-GFP* larvae. Anti-GFP antibody was used to reveal cher-90-GFP. (C) cher-240 with Venus insertion colocalizes with CryAB in Z-bands. (D) Accumulations of cher-90 overexpressed in larval muscles coincide with increased levels of CryAB (arrows), confirming interactions between the two proteins *in vivo*. (E) Muscle-targeted attenuation of *cheerio* leads to the fuzzy sarcomeric actin pattern (asterisks) and to the loss of Z-band-associated localization of CryAB. Note the CryAB aggregates (arrows) that coincide with the fuzzy actin pattern (asterisk). The boxed region is shown at higher magnification to the right. Scale bars: 10 µm in C; 20 µm in D,E.

control flies (Fig. 6E). The heart period was strongly reduced in young flies (Fig. 6B,E) and continued to be significantly shortened in aged *Hand>CryAB-RNAi* animals (data not shown). The shortened heart periods in *CryAB*-attenuated flies were mainly due to decreased diastolic and systolic intervals (Fig. 6E; supplementary material Fig. S6). Conversely, the heart periods of flies overexpressing the wild-type or R120G form of CryAB were unaffected or only slightly (non-significantly) decreased (Fig. 6B).

However, heart-specific expression of $CryAB^{R120G}$ led to a significant increase of arrhythmia in 1-week-old flies (Fig. 6C), a phenotype similar to that observed in transgenic *Drosophila* lines expressing the mutated form of human *CRYAB* in the heart (Xie et al., 2013). Additionally, altering the expression of *CryAB* or introducing $CryAB^{R120G}$ in the heart resulted in enlarged heart diameter (Fig. 6D; supplementary material Fig. S6) and significantly reduced the fractional shortening in $CryAB^{R120G}$ flies, impairing systolic function (supplementary material Fig. S6). Thus, this analysis reveals a novel role of CryAB in the regulation of heartbeat and demonstrates that introducing the R120G mutation into *Drosophila* CryAB leads to pathological cardiac arrhythmia and mimics cardiac defects observed in DRM patients.

CryAB interacts with Cheerio in larval muscles

The altered Cheerio pattern in larval muscles with attenuated *CryAB* prompted us to test whether these two proteins physically interact. We first performed a co-IP experiment with anti-CryAB antibody followed by proteomics analyses. Peptide sequencing of co-immunoprecipitated proteins ranging from 30 to 170 kDa revealed that not only actin but also Tropomyosin 1 and 2 and a few other sarcomeric components, including α-Actinin, Myosin heavy chain and Paramyosin, were strongly represented in CryAB-containing protein complexes (supplementary material Table S1). Importantly, mass spectrometry data also revealed nine matches in Cheerio, corresponding to six different peptides all located in the C-terminal

Development (2015) 142, 994-1005 doi:10.1242/dev.115352

region of the protein (Fig. 7A). *cheerio* (*cher*) is the *Drosophila* homolog of human filamin (Sokol and Cooley, 1999) and encodes several isoforms ranging from 90 to ~260 kDa, all of which are present in third instar larvae (Fig. 7B). The cher-90 isoform is devoid of an ABD and the Rod1 repeat region, and is made up of the C-terminal part of cher-240 (Fig. 7A). Since all the identified peptide sequences matched this common C-terminal part, each Cheerio isoform can potentially interact with CryAB.

To confirm the proteomics data, we performed co-IP experiments with anti-CryAB antibody using protein extracts from the dissected third instar larvae expressing GFP-tagged cher-90 in muscles. We found that immunoprecipitated CryAB protein complexes did indeed contain Cheerio (Fig. 7B). We also tested whether CryAB colocalized with cher-240 in sarcomeres using the $cher^{CPTI0847}$ line, which carries a Venus insertion that does not affect *cheerio* function (Huelsmann et al., 2013). We observed that Venus-tagged Cheerio colocalized at the level of Z-bands with CryAB (Fig. 7C). Moreover, when we overexpressed cher-90-GFP in muscles, it colocalized with CryAB (Fig. 7D), supporting the view that CryAB interacts with Cheerio. Importantly, Cheerio not only interacts with CryAB but also appears to stabilize sarcomeric cytoarchitecture in a manner similar to that of CryAB: knockdown of *cheerio* leads to the fuzzy actin pattern associated with the aggregate-like accumulations of CryAB (Fig. 7E).

To test functional relationships between CryAB and Cheerio we generated a double *UAS-cherRNAi;UAS-CryABRNAi* line that allows attenuation of both genes simultaneously and a rescue line by combining the *UAS-cherRNAi* line with *UAS-CryAB*. The sarcomeric actin pattern in *cheerio CryAB* double-knockdown muscles is severely affected, with areas of weak phalloidin staining complemented by an abnormal Z-band-associated accumulation of Kettin (Sallimus – FlyBase) (supplementary material Fig. S7A-A″), a phenotype that has not been observed in a simple *CryAB-RNAi* context (Fig. 4B). Targeted overexpression of CryAB in muscles with attenuated *cheerio* partially rescues proper sarcomeric actin organization and fully restores the normal Kettin pattern (supplementary material Fig. S7B-B″). Thus, CryAB and Cheerio not only bind to each other but also interact genetically to stabilize sarcomeric and, potentially, perinuclear actin. Altogether, these experiments show that CryAB-Cheerio interactions are crucial for the maintenance of the contractile apparatus in muscles and suggest that loss of this interaction contributes to the muscle defects and affected muscle performance observed in *CryAB-RNAi* larvae.

It has been demonstrated that unfolded filamin interacts with *Drosophila*/mammalian co-chaperone Starvin/BAG3, which plays an important role in the maintenance of Z-disk components (Arndt et al., 2010). We tested whether knocking down *starvin* in muscles influences CryAB sarcomeric localization. The attenuation of *starvin* led to Z-band breaks and an irregular sarcomeric actin pattern associated with clustering of myonuclei (supplementary material Fig. S8). However, the CryAB sarcomeric pattern and perinuclear localization appeared unaffected (supplementary material Fig. S8), supporting a view that CryAB-Cheerio and Starvin-Cheerio interact independently. Since the CRYAB-filamin C interaction has not as yet been tested in vertebrate skeletal muscles, whether this interaction is a conserved feature of CryAB proteins remains to be elucidated.

DISCUSSION

The physiological response to stressful conditions in muscle tissue involves high-molecular-mass Hsps such as Hsp70 (McArdle et al., 2004), together with a set of sHsps (Koh and Escobedo, 2004; Haslbeck et al., 2005). However, besides this classical role, in recent years stress-independent and tissue-specific expression and function have been reported for several members of the Hsp gene family (Michaud and Tanguay, 2003; Rupik et al., 2011).

Here, we provide evidence that in *Drosophila*, the sHsp subfamily member *CryAB* [which is also known as *l(2)efl* (Kurzik-Dumke and Lohmann, 1995)], which encodes the fruit fly ortholog of mammalian CRYAB, is specifically expressed in developing larval somatic muscles and is required for myofibril integrity and muscle performance.

The tissue-specific expression and subcellular localization of CryAB are reminiscent of its vertebrate counterpart

In the developing mammalian heart and skeletal muscles, CRYAB and six other sHsps (HSPB1, HSPB2, HSPB3, HSPB6, HSPB7 and HSPB8) are expressed at a relatively high levels (Davidson et al., 2002). It is not known whether all these genes diverged from a common ancestor with developmental functions, but our phylogenetic analysis indicates that two sHsps involved in muscle development, Hspb8 and CryAB, do have a common ancestor. We also showed that, like its vertebrate counterpart (Doran et al., 2007), the fruit fly CryAB displays muscle- and heart-specific expression and accumulates at the level of the Z-bands and around the nuclei. Interestingly, *Drosophila* CryAB is also localized in between the Z-bands and muscle cell membranes and displays a punctate expression pattern that suggests that it might be a component of Z-band-associated protein complexes. It is well known that vertebrate CRYAB is also expressed at the level of Z-bands and, by acting as a chaperone of the type III IF protein desmin, helps to maintain cytoskeletal integrity in skeletal and cardiac muscle cells (Golenhofen et al., 1999). Desmin IFs are mainly associated with Z-bands and interact with other sarcomeric proteins to form a continuous cytoskeletal network that maintains the spatial organization of contractile apparatus (Goldfarb and Dalakas, 2009). However, neither desmin nor vimentin (another type III IF protein) orthologs exist in *Drosophila* (Sparrow and Schöck, 2009), suggesting that other cytoskeletal components of muscle cells replace them functionally to ensure myofibrillar integrity. The subcellular localization of *Drosophila* CryAB strongly suggests that it interacts with sarcomeric components and, in particular, with Z-band-associated proteins, thereby helping to maintain myofibrillar architecture.

Muscle-specific knockdown of *CryAB* reveals its stress-independent role in sarcomeric organization, muscle performance and heart rhythm

Point mutations in human sHsps lead to several aggregation diseases (Clark and Muchowski, 2000). For example, mutations in αA-crystallin (*CRYAA*) lead to cataract (Litt et al., 1998), missense mutations in *HSP27* (*HSPB1*) are associated with Charcot-Marie-Tooth disease (Evgrafov et al., 2004), and point mutations in *CRYAB* cause DRM (Vicart et al., 1998; Sacconi et al., 2012). Yet, the stress-independent functions of individual members of the sHsp gene family have not been systematically assessed in animal models because of functional redundancies and compensation effects. In the case of *Cryab*, mice knocked out for this gene also lack the adjacent *Hspb2* gene and display no obvious developmental defects (Brady et al., 2001). However, as they become older, *Cryab Hspb2* homozygous knockout mice show postural defects and other health problems that appear to stem from progressive myopathy (Brady et al., 2001). For *Drosophila CryAB*, the impact of its loss of function and its lethality have not yet been confirmed.

Development (2015) 142, 994-1005 doi:10.1242/dev.115352

Here, we analyzed the effects of muscle- and heart-targeted knockdown of *Drosophila CryAB* to better evaluate its stress-independent functions. We focused on larval musculature and on the adult heart, and found that attenuation of *CryAB* led to a number of morphological and ultrastructural defects in body wall muscles, impaired muscle performance and accelerated heartbeat. Importantly, muscle alterations lead to local Z-band misalignment, which could be responsible for the observed muscle fiber splitting. Affected myofibrillar integrity results in a markedly altered contractility index in *Mef2>CryAB-RNAi* larvae, which also display lower motility compared with age-matched wild-type individuals. The sarcomeric alterations are also associated with the clustering/mislocalization of nuclei in muscle fibers and with abnormal swelling of mitochondria, together revealing the important developmental role of CryAB in *Drosophila* in the maintenance of correct muscle function and structural integrity. Some of the phenotypes resulting from the muscle-specific attenuation of *Drosophila CryAB*, including disruption of myofibrillar organization and muscle weakness, are reminiscent of those observed in myofibrillar myopathies in human (Goldfarb and Dalakas, 2009).

Body wall and cardiac muscle alterations in larvae expressing CryAB with the R120G mutation

In human pathological cases, when the IF network does not assemble correctly and creates aggregates, CRYAB can reorganize the malfolded IF proteins into a normal filamentous network (Koyama and Goldman, 1999). Some mutations in *CRYAB*, such as R120G (Vicart et al., 1998) or D109H, are claimed to affect dimerization of the protein (Sacconi et al., 2012) leading to loss of its chaperone activity and ultimately to pathological muscle defects. Interestingly, protein sequence alignment revealed that both these residues (R120 and D109) are conserved in *Drosophila* CryAB. When we generated a *Drosophila* strain carrying a mutation in one of these residues, $CryAB^{R120G}$, we found that in larval muscle cells with accumulations of $CryAB^{R120G}$ the sarcomeric architecture and, in particular, the actin filament pattern were severely affected. We also observed a misalignment of myofibrils and the appearance of protein aggregates containing $CryAB^{R120G}$, symptoms also seen in DRM patients (Goldfarb and Dalakas, 2009). The affected myofibrillar integrity and irregular sarcomeric pattern correlated with reduced muscle performance as measured by motility assays in $Mef2>CryAB^{R120G}$ third instar larvae. Taken together, these observations suggest that the R120G mutation in *Drosophila* CryAB has an impact on larva body wall muscles similar to that which the analogous mutation in CRYAB has on human skeletal muscles leading to disruption of myofibrillar integrity and muscle weakness. In DRM patients carrying the $CRYAB^{R120G}$ mutation, muscle defects appear in mid-age adults, whereas in our *Drosophila* model, following forced expression of $CryAB^{R120G}$ in muscles, they are apparent in third instar larva. At this late stage of larval development muscles are fully functional and differentiated, like those in adult humans.

Another important phenotype observed in patients carrying the R120G mutation in CRYAB is increased systolic heart diameter, dilated cardiomyopathy and arrhythmia. Here again, targeted cardiac expression of $CryAB^{R120G}$ resulted in arrhythmic heart beating in the adult fly, reminiscent of that observed in the DRM mouse model and in DRM patients (Wang et al., 2001).

Thus, expressing the R120G-mutated form of CryAB in body wall or in cardiac muscles in *Drosophila* leads to pathological defects similar to those observed in patients harboring the $CRYAB^{R120G}$ mutation. This suggests that this mutation, which potentially impairs CryAB dimerization (Sacconi et al., 2012), might have a more general impact on the chaperone function of CryAB and not only on interactions with desmin IFs.

Cheerio and other potential CryAB-interacting proteins in *Drosophila* muscles

As reported above, muscle-specific expression of *Drosophila* $CryAB^{R120G}$ leads to DRM-like phenotypes with Z-band disruption and adversely affected muscle performance. However, as revealed by sequencing of the *Drosophila* genome (Adams et al., 2000), no gene orthologous to desmin has been identified in the fruit fly, suggesting that CryAB interacts with other sarcomeric components to stabilize the contractile apparatus. To identify potential CryAB-interacting proteins we performed co-IP experiments using dissected third instar larvae. Highly enriched sarcomeric proteins bound by CryAB include actins, Tropomyosin 1 and 2, α-Actinin, Paramyosin, Myosin heavy chain and Cheerio.

Drosophila CryAB accumulates in Z-bands and to a lesser extent in M-lines, and thus can potentially interact with all these sarcomeric components. Identifying actin in the IP material is consistent with the fact that CryAB has an ABD and that the actin pattern is affected in muscle fibers with attenuated *CryAB* as it is in muscles expressing CryAB carrying a mutation in the ABD. However, the finding that CryAB can potentially interact with Z-band-associated Cheerio was of particular interest, as in humans mutations in filamin C lead to myofibrillar myopathy with dissolution of myofibrils similar to that observed in DRM (Kley et al., 2007; Luan et al., 2010). Filamins are actin-crosslinking proteins consisting of an N-terminal ABD followed by 24 immunoglobulin-like repeats (Stossel et al., 2001) and are involved in a number of cellular processes including cell-matrix adhesion, mechanoprotection and actin remodeling (Feng and Walsh, 2004). In vertebrates, filamin C is muscle specific and localizes at myotendinous junctions and also at Z-bands and costameres (Ohashi et al., 2005; van der Ven et al., 2000a,b). It has been shown that filamin C interacts with two major protein complexes at the sarcolemma, namely the dystrophin-associated glycoprotein complex (DGC) (Thompson et al., 2000) and the integrin complex (Gontier et al., 2005; Loo et al., 1998), both of which are known to have important roles in affording mechanical integrity to striated muscle. However, through its C-terminal region, filamin C also binds the Z-band proteins myotilin (van der Ven et al., 2000b) and myopodin (synaptopodin 2) (Linnemann et al., 2010), suggesting that it ensures a link between Z-bands and sarcolemmal DGC and integrin complexes, thus maintaining the mechanical integrity of muscle cells. This possibility is supported by the detachment of myofibrils from sarcolemma and intercalated Z-bands in muscles of *zacro* (*filamin C*) medaka mutants (Fujita et al., 2012). In *Drosophila*, overall filamin protein structure its actin-crosslinking function are conserved in Cheerio. It plays a key role in ring canal formation during oogenesis (Sokol and Cooley, 1999) and is involved in the positioning of nuclei in ovarian nurse cells (Huelsmann et al., 2013), but the role of Cheerio in muscles had remained elusive.

Here, we show that in third instar larval muscles Cheerio protein accumulates between myofibrils and the muscle cell membrane at the level of Z-bands and around the nuclei, a subcellular localization reminiscent of that of filamin C. We also found that the sarcomeric Cheerio pattern was disrupted in larvae with attenuated *CryAB*, suggesting that the identified interactions between CryAB and Cheerio might help to maintain myofibrillar integrity. Thus, we hypothesize that CryAB exerts a chaperone function on Cheerio in

Development (2015) 142, 994-1005 doi:10.1242/dev.115352

Drosophila muscles, which are devoid of desmin IFs, and that this interaction helps to stabilize the contractile apparatus.

Recently, it was reported that the conserved BAG3/Starvin complex detects mechanical unfolding of filamins caused by cell stretching (Arndt et al., 2010; Ulbricht et al., 2013). This complex binds unfolded filamins and targets them to autophagosomes for degradation. It is unclear whether *Drosophila* CryAB is part of the same complex or of another sHsp complex that regulates filamin and muscle cell function. The fact that *Drosophila* CryAB can interact with cher-90, the Cheerio isoform that does not contain an ABD and thus might not be stretched and mechanically opened up, suggests that the CryAB complex might bind the folded C-terminus of Cheerio and thus not be part of the BAG3/Starvin complex. Future experiments are required to determine whether the CryAB and BAG3/Starvin complexes bound to filamins have overlapping or specific roles during the development and function of skeletal and cardiac muscle cells.

These findings raise the question as to the extent to which Cheerio is able to replace the IF network in *Drosophila* muscles. Human CRYAB is known to interact with desmin (Goldfarb and Dalakas, 2009), with sarcomeric actin (Bennardini et al., 1992) and with titin (Golenhofen et al., 2002); however, whether the identified interaction between *Drosophila* CryAB and Cheerio is conserved in human muscles and, if so, whether it helps to stabilize myofibrillar architecture remains to be elucidated.

MATERIALS AND METHODS

Drosophila stocks

The following *Drosophila* stocks were used: w^{1118} strain as wild type; *Mef2-Gal4* [Bloomington Stock Center (BSC) BL27390]; *Hand-Gal4* (kindly provided by L. Perrin, TAGC, Marseille, France); *UAS-lacZ* (BSC, BL1776); *UAS-RNAi-cher* [Vienna Drosophila RNAi Center (VDRC) 107451]; *UAS-RNAi-starvin* (VDRC 42564); two *UAS-RNAi-CryAB* lines (VDRC 40532 and 107305); *cherCPTI0847* protein trap line [Kyoto Drosophila Genomics Resource Center (DGRC)]; and *UASp-cher90-GFP* (generated by S. Huelsmann, Gurdon Institute, Cambridge, UK). The *UASp-Venus-CryAB*, *UASp-Venus-CryAB ABDmut* and *UASp-Venus-CryAB R120G* lines were generated in the K.J. lab. The generation of *CryAB* and *cheerio* transgenic lines is described in the supplementary Materials and Methods.

Antibodies and fluorescent markers

Primary antibodies: goat anti-GFP (1:500; Abcam, ab5450); rat anti-CryAB (1:500; generated in the K.J. lab); rabbit anti-Mef2 (1:1000; gift from H. Nguyen, Erlangen University, Germany); rat anti-Kettin (1:25; Abcam, ab50585); mouse anti-LamC28.26 [1:1000; Developmental Studies Hybridoma Bank (DSHB)]; rabbit anti-β3-tubulin (1:10,000; gift from R. Renkawitz-Pohl, Marburg University, Germany); mouse anti-β-actin (1:10; Invitrogen, AC-15); guinea pig anti-Msp300 (1:300; gift from T. Volk, Weitzmann Institute, Israel); rat anti-Cheerio (1:200; Sokol and Cooley, 1999); and rabbit anti-active Caspase 3 (1:1000; Abcam, ab13847). We also used different secondary fluorescent antibodies as well as 18 nm colloidal gold-AffiniPure goat anti-rat IgG (whole molecule) (Jackson ImmunoResearch; 1:20) and 10 nm goat anti-rat IgG (whole molecule)-gold (Sigma-Aldrich; 1:100) conjugated to Alexa Fluor 488, CY3 or CY5 (1:300; Jackson ImmunoResearch). Phalloidin-TRITC (1:1000; Sigma) was used for revealing sarcomeric actin.

RT-PCR analysis of *CryAB* gene attenuation

Analyses of *CryAB* transcript levels after RNAi-based attenuation are described in the supplementary Materials and Methods.

Phenotypic analyses

Tests of larval viability and muscle performance using the righting, motility and journey tests, and characterization of muscle morphology and heart physiology are described in the supplementary Materials and Methods. The heart physiology assay was performed as described previously (Fink et al. 2009).

Immunofluorescence staining of larval muscles and adult fly heart

Third instar larvae were dissected as described previously (Budnik et al., 2006) in ice-cold Ca^{2+}-free saline buffer containing 128 mM NaCl, 2 mM KCl, 4 mM $MgCl_2$, 1 mM EGTA, 35 mM sucrose and 5 mM HEPES pH 7.2 (Demontis and Perrimon, 2009). Buffer without EGTA was used for measurements of contracted muscles. Body wall muscles were fixed with 4% formaldehyde in PBS for 15 min and then rinsed three times for 5 min each in PBS with 0.5% Tween 20 (PBT). Muscles were blocked for 30 min in 20% horse serum in PBT at room temperature. Dissection and staining of adult flies were performed as described previously (Taghli-Lamallem et al., 2008). Primary antibodies were applied overnight at 4°C. After three washes in PBT, secondary antibodies were applied for 2 h at room temperature with or without phalloidin-TRITC as appropriate. MitoTracker Red CMXRos (Invitrogen) was used at 1.5 µM in ice-cold Ca^{2+}-free saline buffer; it was incubated for 15 min at 37°C with dissected larvae. Subsequently, larvae were fixed in 4% formaldehyde for 15 min and washed in PBS three times for 10 min each. Muscle and heart preparations were mounted in Fluoromount-G anti-fade reagent (Southern Biotech) and analyzed using SP5 or SP8 (Leica) confocal microscopes. 3D models of labeled muscles were generated using Imaris software (Bitplane).

Transmission electron microscopy (TEM)

TEM of dissected larvae and immunogold detection of CryAB in TEM sections are described in the supplementary Materials and Methods.

CryAB interactions by co-IP and mass spectrometry

For the co-IP assay, 300 dissected and frozen *Mef2>cher90-GFP* (for CryAB-Cheerio) or w^{1118} (for CryAB-Msp300) larvae were homogenized at 4°C in 500 µl HEB extraction buffer [containing 50 mM Tris (pH 7.6), 140 mM NaCl, 5 mM EDTA, 1% (V/V) NP40 and 0.5% (W/V) sodium deoxycholate] as described previously (Perng et al., 2006) and supplemented with a protease inhibitor cocktail (Roche). After 30 min incubation on ice, lysate was centrifuged at 17,000 ***g*** for 10 min at 4°C. Supernatant was pre-absorbed 1 h at 4°C with 50 µl protein G-Sepharose (Amersham) to eliminate non-specific binding of the proteins to the beads. The protein G-Sepharose beads were separated from the lysate by centrifugation 1 min at 13,000 ***g*** at 4°C. The supernatant was incubated 4 h at 4°C with 5 µl rat anti-CryAB antibody or with 5 µl rat non-immune serum as a negative control. The protein G-Sepharose was subsequently added to each lysate/antibody mixture and incubated overnight at 4°C with gentle agitation. The complexes were then washed three times with washing buffer (50 mM Tris-HCl pH 7.5, 500 mM NaCl, 0.1% NP40) and proteins eluted by boiling the beads in 2× SDS-PAGE buffer for 10 min. Eluted proteins were separated on a 4-10% SDS-PAGE gradient gel and blotted to PDF membrane (Whatman), blocked with 5% non-fat milk. The membrane was incubated with anti-GFP antibody (1:5000; for CryAB-Cheerio) or with anti-Msp300 (1:1000; for CryAB-Msp300) followed by anti-mouse or anti-guinea pig HRP-conjugated secondary antibody (1:10,000) at 25°C for 1 h, and subsequently washed three times with TBST (TBS containing 0.5% Tween-20). Protein bands were visualized using the ECL detection kit (Amersham) and analyzed with the Chemi Doc imaging system (Bio-Rad).

Mass spectrometry to identify CryAB-interacting proteins is described in the supplementary Materials and Methods.

Bioinformatics

Bioinformatics analysis of phylogenic relationships among sHsps is described in the supplementary Materials and Methods.

Acknowledgements

We thank H. Nguyen, T. Volk, R. Renkawitz-Pohl, B. Suter, L. Cooley, the BSC, VDRC and DGRC for providing reagents and fly stocks; Fly-Facility for generation of *CryAB* transgenic stocks; and J. Overton for injection of the *cheerio* construct.

Competing interests
The authors declare no competing or financial interests.

Author contributions
I.W. and T.J. designed the study; I.W., J.J., M.Z., O.T.-L., Y.R., M.D. and G.J. performed the research and analyzed the data; Y.R. performed bioinformatics analyses; I.W. and M.D. analyzed EM muscle preparations; S.H. provided cheerio alleles; I.W., S.H., K.J. and T.J. wrote the paper.

Funding
This work was supported by Agence Nationale de la Recherche (ANR) grants MYO-ID and ID-CELL-SPE, an Infrastructure TEFOR grant, an Equipe Fondation pour la Recherche Médicale (FRM) grant and Association Française Contre les Myopathies (AFM) grants to K.J.

Supplementary material
Supplementary material available online at
http://dev.biologists.org/lookup/suppl/doi:10.1242/dev.115352/-/DC1

References

Adams, M.D., Celniker, S.E., Holt, R.A., Evans C.A., Gocayne, J.D. et al. (2000). The genome sequence of *Drosophila melanogaster*. *Science* **287**, 2185-2195.
Arndt, V., Dick, N., Tawo, R., Dreiseidler M., Wenzel, D., Hesse, M., Fürst, D. O., Saftig, P., Saint, R., Fleischmann, B. K. et al. (2010). Chaperone-assisted selective autophagy is essential for muscle maintenance. *Curr. Biol.* **20**, 143-148.
Bate M. (1990). The embryonic development of larval muscles in Drosophila. *Development* **110**, 791-804.
Bennardini F., Wrzosek A. and Chiesi M. (1992). Alpha-B crystallin in cardiac tissue. Association with actin and desmin filaments. *Circ. Res.* **71**, 288-294.
Brady, J. P., Garland, D. L., Green, D. E., Tamm, E. R., Giblin, F. J. and Wawrousek, E. F. (2001). AlphaB-crystallin in lens development and muscle integrity: a gene knockout approach. *Invest. Ophthalmol. Vis. Sci.* **42**, 2924-2934.
Budnik, V., Gorczyca, M. and Prokop, A. (2006). Selected methods for the anatomical study of Drosophila embryonic and larval neuromuscular junctions. *Int. Rev. Neurobiol.* **75**, 323-365.
Clark, J. I. and Muchowski, P. J. (2000). Small heat-shock proteins and their potential role in human disease. *Curr. Opin. Struct. Biol.* **10**, 52-59.
Colinet, H., Lee, S. F. and Hoffmann, A. (2010). Temporal expression of heat shock genes during cold stress and recovery from chill coma in adult Drosophila melanogaster. *FEBS J.* **277**, 174-185.
Corces, V., Holmgren, R., Freund, R., Morimoto, R. and Meselson, M. (1980). Four heat shock proteins of Drosophila melanogaster coded within a 12-kilobase region in chromosome subdivision 67B. *Proc. Natl. Acad. Sci. USA* **77**, 5390-5393.
Dalakas, M. C., Park, K.-Y., Semino-Mora, C., Lee, H. S., Sivakumar, K. and Goldfarb, L. G. (2000). Desmin myopathy, a skeletal myopathy with cardiomyopathy caused by mutations in the desmin gene. *N. Engl. J. Med.* **342**, 770-780.
Davidson, S. M., Loones, M.-T., Duverger, O. and Morange, M. (2002). The developmental expression of small HSP. *Prog. Mol. Subcell. Biol.* **28**, 103-128.
Demontis, F. and Perrimon, N. (2009). Integration of Insulin receptor/Foxo signaling and dMyc activity during muscle growth regulates body size in Drosophila. *Development* **136**, 983-993.
Doran, P., Gannon, J., O'Connell, K. and Ohlendieck, K. (2007). Aging skeletal muscle shows a drastic increase in the small heat shock proteins alphaB-crystallin/HspB5 and cvHsp/HspB7. *Eur. J. Cell Biol.* **86**, 629-640.
Dubin, R. A., Ally, A. H., Chung, S. and Piatigorsky, J. (1990). Human alpha B-crystallin gene and preferential promoter function in lens. *Genomics* **7**, 594-601.
Evgrafov, O. V., Mersiyanova, I., Irobi, J., Van Den Bosch, L., Dierick, I., Leung, C. L., Schagina, O., Verpoorten, N., Van Impe, K., Fedotov, V. et al. (2004). Mutant small heat-shock protein 27 causes axonal Charcot-Marie-Tooth disease and distal hereditary motor neuropathy. *Nat. Genet.* **36**, 602-606.
Feng, Y. and Walsh, C. A. (2004). The many faces of filamin: a versatile molecular scaffold for cell motility and signalling. *Nat. Cell Biol.* **6**, 1034-1038.
Fink, M., Callol-Massot, C., Chu, A., Ruiz-Lozano, P., Izpisua Belmonte, J. C., Giles, W., Bodmer, R. and Ocorr, K. (2009). A new method for detection and quantification of heartbeat parameters in Drosophila, zebrafish, and embryonic mouse hearts. *Biotechniques* **46**, 101-113.
Flatt, T., Min, K.-J., D'Alterio, C., Villa-Cuesta, E., Cumbers, J., Lehmann, R., Jones, D. L. and Tatar, M. (2008). Drosophila germ-line modulation of insulin signaling and lifespan. *Proc. Natl. Acad. Sci. USA* **105**, 6368-6373.
Fujita, M., Mitsuhashi, H., Isogai, S., Nakata, T., Kawakami, A., Nonaka, I., Noguchi, S., Hayashi, Y. K., Nishino, I. and Kudo, A. (2012). Filamin C plays an essential role in the maintenance of the structural integrity of cardiac and skeletal muscles, revealed by the medaka mutant zacro. *Dev. Biol.* **361**, 79-89.
Goldfarb, L. G. and Dalakas, M. C. (2009). Tragedy in a heartbeat: malfunctioning desmin causes skeletal and cardiac muscle disease. *J. Clin. Invest.* **119**, 1806-1813.
Goldfarb, L. G., Vicart, P., Goebel, H. H. and Dalakas, M. C. (2004). Desmin myopathy. *Brain* **127**, 723-734.
Golenhofen, N., Htun, P., Ness, W., Koob, R., Schaper, W. and Drenckhahn, D. (1999). Binding of the stress protein alpha B-crystallin to cardiac myofibrils correlates with the degree of myocardial damage during ischemia/reperfusion in vivo. *J. Mol. Cell. Cardiol.* **31**, 569-580.
Golenhofen N., Arbeiter A., Koob R. and Drenckhahn D. (2002). Ischemia-induced association of the stress protein alpha-B crystallin with I-band portion of cardiac titin. *J. Mol. Cell. Cardiol.* **34**, 309-319.
Gontier, Y., Taivainen, A., Fontao, L., Sonnenberg, A., van der Flier, A., Carpen, O., Faulkner, G. and Borradori, L. (2005). The Z-disc proteins myotilin and FATZ-1 interact with each other and are connected to the sarcolemma via muscle-specific filamins. *J. Cell Sci.* **118**, 3739-3749.
Haslbeck, M., Franzmann, T., Weinfurtner, D. and Buchner, J. (2005). Some like it hot: the structure and function of small heat-shock proteins. *Nat. Struct. Mol. Biol.* **12**, 842-846.
Huelsmann, S., Ylänne, J. and Brown, N. H. (2013). Filopodia-like actin cables position nuclei in association with perinuclear actin in Drosophila nurse cells. *Dev. Cell* **26**, 604-615.
Ingolia, T. D. and Craig, E. A. (1982). Four small Drosophila heat shock proteins are related to each other and to mammalian alpha-crystallin. *Proc. Natl. Acad. Sci. USA* **79**, 2360-2364.
Kley, R. A., Hellenbroich, Y., van der Ven, P. F. M., Furst, D. O., Huebner, A., Bruchertseifer, V., Peters, S. A., Heyer, C. M., Kirschner, J., Schroder, R. et al. (2007). Clinical and morphological phenotype of the filamin myopathy: a study of 31 German patients. *Brain* **130**, 3250-3264.
Koh, T. J. and Escobedo, J. (2004). Cytoskeletal disruption and small heat shock protein translocation immediately after lengthening contractions. *Am. J. Physiol. Cell Physiol.* **286**, C713-C722.
Koyama, Y. and Goldman, J. E. (1999). Formation of GFAP cytoplasmic inclusions in astrocytes and their disaggregation by alphaB-crystallin. *Am. J. Pathol.* **154**, 1563-1572.
Kurzik-Dumke, U. and Lohmann, E. (1995). Sequence of the new Drosophila melanogaster small heat-shock-related gene, lethal(2) essential for life [l(2)efl], at locus 59F4,5. *Gene* **154**, 171-175.
Lindquist, S. and Craig, E. A. (1988). The heat-shock proteins. *Annu. Rev. Genet.* **22**, 631-677.
Linnemann, A., van der Ven, P. F. M., Vakeel, P., Albinus, B., Simonis, D., Bendas, G., Schenk, J. A., Micheel, B., Kley, R. A. and Fürst, D. O. (2010). The sarcomeric Z-disc component myopodin is a multiadapter protein that interacts with filamin and alpha-actinin. *Eur. J. Cell Biol.* **89**, 681-692.
Litt, M., Kramer, P., LaMorticella, D. M., Murphey, W., Lovrien, E. W. and Weleber, R. G. (1998). Autosomal dominant congenital cataract associated with a missense mutation in the human alpha crystallin gene CRYAA. *Hum. Mol. Genet.* **7**, 471-474.
Loo, M. A., Jensen, T. J., Cui, L., Hou, Y.-x., Chang, X.-B. and Riordan, J. R. (1998). Perturbation of Hsp90 interaction with nascent CFTR prevents its maturation and accelerates its degradation by the proteasome. *EMBO J.* **17**, 6879-6887.
Luan, X., Hong, D., Zhang, W., Wang, Z. and Yuan, Y. (2010). A novel heterozygous deletion–insertion mutation (2695–2712 del/GTTTGT ins) in exon 18 of the filamin C gene causes filaminopathy in a large Chinese family. *Neuromuscul. Disord.* **20**, 390-396.
Marin, R. and Tanguay, R. M. (1996). Stage-specific localization of the small heat shock protein Hsp27 during oogenesis in Drosophila melanogaster. *Chromosoma* **105**, 142-149.
McArdle, A., Dillmann, W. H., Mestril, R., Faulkner, J. A. and Jackson, M. J. (2004). Overexpression of HSP70 in mouse skeletal muscle protects against muscle damage and age-related muscle dysfunction. *FASEB J.* **18**, 355-357.
McWilliam, H., Li, W., Uludag, M., Squizzato, S., Park, Y. M., Buso, N., Cowley, A. P. and Lopez, R. (2013). Analysis tool web services from the EMBL-EBI. *Nucleic Acids Res.* **41**, W597-W600.
Metzger, T., Gache, V., Xu, M., Cadot, B., Folker, E. S., Richardson, B. E., Gomes, E. R. and Baylies, M. K. (2012). MAP and kinesin-dependent nuclear positioning is required for skeletal muscle function. *Nature* **484**, 120-124.
Michaud, S. and Tanguay, R. M. (2003). Expression of the Hsp23 chaperone during Drosophila embryogenesis: association to distinct neural and glial lineages. *BMC Dev. Biol.* **3**, 9.
Morimoto, R. I. (1998). Regulation of the heat shock transcriptional response: cross talk between a family of heat shock factors, molecular chaperones, and negative regulators. *Genes Dev.* **12**, 3788-3796.
Morrow, G. and Tanguay, R. M. (2003). Heat shock proteins and aging in Drosophila melanogaster. *Semin. Cell Dev. Biol.* **14**, 291-299.
Mymrikov, E. V., Seit-Nebi, A. S. and Gusev, N. B. (2010). Large potentials of small heat shock proteins. *Physiol. Rev.* **91**, 1123-1159.
Nicholl, I. D. and Quinlan, R. A. (1994). Chaperone activity of alpha-crystallins modulates intermediate filament assembly. *EMBO J.* **13**, 945-953.
Ohashi, K., Oshima, K., Tachikawa, M., Morikawa, N., Hashimoto, Y., Ito, M., Mori, H., Kuribayashi, T. and Terasaki, A. G. (2005). Chicken gizzard filamin, retina filamin and cgABP260 are respectively, smooth muscle-, non-muscle- and

pan-muscle-type isoforms: distribution and localization in muscles. *Cell Motil. Cytoskeleton* **61**, 214-225.

Perng, M. D., Wen, S. F., van den Ijssel, P., Prescott, A. R. and Quinlan, R. A. (2004). Desmin aggregate formation by R120G alphaB-crystallin is caused by altered filament interactions and is dependent upon network status in cells. *Mol. Biol. Cell* **15**, 2335-2346.

Perng, M. D., Su, M., Wen Fang, S., Li, R., Gibbon, T., Prescott, A. R., Brenner, M. and Quinlan, R. A. (2006). The Alexander disease-causing glial fibrillary acidic protein mutant, R416W, accumulates into Rosenthal fibers by a pathway that involves filament aggregation and the association of αB-crystallin and HSP27. *Am. J. Hum. Genet.* **79**, 197-213.

Picard, M., Hepple, R. T. and Burelle, Y. (2012). Mitochondrial functional specialization in glycolytic and oxidative muscle fibers: tailoring the organelle for optimal function. *Am. J. Physiol. Cell Physiol.* **302**, C629-C641.

Rupik, W., Jasik, K., Bembenek, J. and Widłak, W. (2011). The expression patterns of heat shock genes and proteins and their role during vertebrate's development. *Comp. Biochem. Physiol. A Mol. Integr. Physiol.* **159**, 349-366.

Sacconi, S., Féasson, L., Antoine, J. C., Pécheux, C., Bernard, R., Cobo, A. M., Casarin, A., Salviati, L., Desnuelle, C. and Urtizberea, A. (2012). A novel CRYAB mutation resulting in multisystemic disease. *Neuromuscul. Disord.* **22**, 66-72.

Simon, S., Fontaine, J.-M., Martin, J. L., Sun, X., Hoppe, A. D., Welsh, M. J., Benndorf, R. and Vicart, P. (2007). Myopathy-associated alphaB-crystallin mutants: abnormal phosphorylation, intracellular location, and interactions with other small heat shock proteins. *J. Biol. Chem.* **282**, 34276-34287.

Sokol, N. S. and Cooley, L. (1999). Drosophila filamin encoded by the cheerio locus is a component of ovarian ring canals. *Curr. Biol.* **9**, 1221-1230.

Sorensen, J. G., Kristensen, T. N. and Loeschcke, V. (2003). The evolutionary and ecological role of heat shock proteins. *Ecol. Lett.* **6**, 1025-1037.

Sparrow, J. C. and Schöck, F. (2009). The initial steps of myofibril assembly: integrins pave the way. *Nat. Rev. Mol. Cell Biol.* **10**, 293-298.

Stossel, T. P., Condeelis, J., Cooley, L., Hartwig, J. H., Noegel, A., Schleicher, M. and Shapiro, S. S. (2001). Filamins as integrators of cell mechanics and signalling. *Nat. Rev. Mol. Cell Biol.* **2**, 138-145.

Sugiyama, Y., Suzuki, A., Kishikawa, M., Akutsu, R., Hirose, T., Waye, M. M. Y., Tsui, S. K. W., Yoshida, S. and Ohno, S. (2000). Muscle develops a specific form of small heat shock protein complex composed of MKBP/HSPB2 and HSPB3 during myogenic differentiation. *J. Biol. Chem.* **275**, 1095-1104.

Taghli-Lamallem, O., Akasaka, T., Hogg, G., Nudel, U., Yaffe, D., Chamberlain, J. S., Ocorr, K. and Bodmer, R. (2008). Dystrophin deficiency in Drosophila reduces lifespan and causes a dilated cardiomyopathy phenotype. *Aging Cell* **7**, 237-249.

Thompson, T. G., Chan, Y.-M., Hack, A. A., Brosius, M., Rajala, M., Lidov, H. G. W., McNally, E. M., Watkins, S. and Kunkel, L. M. (2000). Filamin 2 (FLN2): a muscle-specific sarcoglycan interacting protein. *J. Cell Biol.* **148**, 115-126.

Ulbricht, A., Eppler, F. J., Tapia, V. E., van der Ven, P. F. M., Hampe, N., Hersch, N., Vakeel, P., Stadel, D., Haas, A., Saftig, P. et al. (2013). Cellular mechanotransduction relies on tension-induced and chaperone-assisted autophagy. *Curr. Biol.* **23**, 430-435.

van der Ven, P. F. M., Wiesner, S., Salmikangas, P., Auerbach, D., Himmel, M., Kempa, S., Hayess, K., Pacholsky, D., Taivainen, A., Schröder, R. et al. (2000a). Indications for a novel muscular dystrophy pathway: gamma-filamin, the muscle-specific filamin isoform, interacts with myotilin. *J. Cell Biol.* **151**, 235-248.

van der Ven, P. F. M., Obermann, W. M. J., Lemke, B., Gautel, M., Weber, K. and Fürst, D. O. (2000b). Characterization of muscle filamin isoforms suggests a possible role of gamma-filamin/ABP-L in sarcomeric Z-disc formation. *Cell Motil. Cytoskeleton* **45**, 149-162.

Vicart, P., Caron, A., Guicheney, P., Li, Z., Prévost, M.-C., Faure, A., Chateau, D., Chapon, F., Tomé, F., Dupret, J.-M. et al. (1998). A missense mutation in the alphaB-crystallin chaperone gene causes a desmin-related myopathy. *Nat. Genet.* **20**, 92-95.

Wang, X., Osinska, H., Klevitsky, R., Gerdes, A. M., Nieman, M., Lorenz, J., Hewett, T. and Robbins, J. (2001). Expression of R120G-alphaB-crystallin causes aberrant desmin and alphaB-crystallin aggregation and cardiomyopathy in mice. *Circ. Res.* **89**, 84-91.

Waterhouse, A. M., Procter, J. B., Martin, D. M. A., Clamp, M. and Barton, G. J. (2009). Jalview Version 2 - a multiple sequence alignment editor and analysis workbench. *Bioinformatics* **25**, 1189-1191.

Xie, H. B., Cammarato, A., Rajasekaran, N. S., Zhang, H., Suggs, J. A., Lin, H.-C., Bernstein, S. I., Benjamin, I. J. and Golic, K. G. (2013). The NADPH metabolic network regulates human αB-crystallin cardiomyopathy and reductive stress in Drosophila melanogaster. *PLoS Genet.* **9**, e1003544.

Zobel, A. T., Loranger, A., Marceau, N., Thériault, J. R., Lambert, H. and Landry, J. (2003). Distinct chaperone mechanisms can delay the formation of aggresomes by the myopathy-causing R120G alphaB-crystallin mutant. *Hum. Mol. Genet.* **12**, 1609-1620.

Supplemental materials and methods

Viability and behavioral tests

In the viability test, 200 embryos were plated on a Petri dish containing 3% agarose supplemented with grape juice and with yeast paste. Subsequently, 1st instar larvae were moved to vials with a standard medium. Individuals, achieving each stage of development (3rd larval instar, pupae, imago) were quantified. Behavioral assays were carried out on fifteen 3rd instar larvae per genotype and repeated 3 times for each individual. For all locomotor assays larvae were placed for at least 120s on a Petri dish filled with solidified 3% agarose for adaptation before being tested. In the righting assay, individuals were placed on a Petri dish with 3% agarose on a dorsal position and the time needed to reverse to a ventral position was measured. For the journey test a 2 mm wide, 5 mm deep and 60 mm long track was created on a Petri dish containing 3% agarose. Fresh yeast paste was placed behind the end line as a stimulus. Larvae were placed on the test track and the time taken to crawl 50 mm distance was recorded. In motility test larvae were crawling on a Petri dish with 3% agarose and the number of peristaltic movements were counted during 30 s.

Muscle morphology measurements

VL3, VL4 and SBM muscles of abdominal segments 3 or 4 were analysed in 15-22 dissected and fixed 3rd instar larvae, as described above. Observations of muscle morphology, as well as measurements of muscle length, diameter, number and size of sarcomeres were carried out on muscles stained with phalloidin. Muscle nuclei were visualized by anti-Mef2 antibody. The fibre contractility index (CI) was calculated from following formula: CI = (size of relaxed fibres – size of contracted fibres)/size of relaxed fibres. FV300 (Olympus) confocal microscope was used for imaging and Fluoview software (Olympus) for muscle measurements. Statistical analyses were carried out using the GraphPad Prism5 software. T-test non-parametric or one-way ANOVA were used for phenotypes comparison. The results are reported on the graphs as a standard error of a mean and $P<0.05$ is considered as statistically significant.

RT-PCR

To obtain *Drosophila* cDNA, total RNA was extracted from 50 3rd instar larvae (WT and Mef> CryAB-RNAi, using a TRIzol reagent (Invitrogen). The remaining DNA was removed by RQ1 DNAse (Promega). 2 µl of each RNA were used for reverse transcription, performed with the Superscript III First strand Synthesis System (Invitrogen) according to manufacturer's instructions. To compare the level of *cryAB* expression in selected fly strains, 2 µl of reverse transcription products (described above) were amplified via PCR, by using following pairs of primers: forward, 5'-TCCGTAGTGCCACTGATGTTC-3' and reverse, 5'-CTAGGCGGTGGAGGTCTCC-3'. As a control *gapdh1* was used, whose expression remains at a constant level. All the DNA amplifications were obtained with a Taq DNA polymerase (Invitrogen) according to manufacturer's instructions.

Heart physiological analysis

Anesthetized flies with fly nap (Carolina Biol., Corp.) were dissected to expose the heart for filming according to previously described protocols (Fink et al., 2009). These beating heart movies were taken at rate of about 130 frames per second using Simple PCI software (Compix, Sewickley, PA). We use MatLab-based image analysis program to quantify and generate cardiac parameters measurements (Fink et al., 2009). M-modes illustrate movements

of the heart tube edges in Y-axis over time in X-axis, generated by excising and aligning a single pixel-wide from successive movie frames. Heart periods are defined as the time between the ends of two consecutive diastolic intervals. We used Prism software–one way ANOVA analysis and Tukey test to perform the statistics on 20 flies for each genotype.

Generation of *UASp-Cher90_GFP* line

To generate *pUASP-Cher90* we cloned a NotI-EcoRI cheerio fragment with an EcoRI-XbaI mGFP6 fragment into the *attB-UASP* vector (kindly provided by Beat Suter) cut NotI-XbaI. We used the following primers to generate the cheerio fragment from the EST RE60544 (DGRC):
ATATATGCGGCCGCATGCCTAGCGGTAAAGTAGACAAACCCGTGAT and
ATATATTCTAGAGAATTCCACATCGATCTGGAATGGGGAGCCGGGTATATGC;
We used the following primers to generate the mGFP6 fragment:
ATATATGAATTCCCCTCGAGCTCATCGATGAGTAAAGGAGAAGAA and
TATATATCTAGATCAAGCTTTGTATAGTTCATCCATG.
The construct was sequenced and integrated into the attP landing site 51D (Bischof et al., 2007).

Generation of *UASp-Venus-dCryAB*, *UASp-Venus-dCryABR120G* and *UASp-Venus-dCryAB ABDmut* lines

For plasmid construction *dCryAB* coding sequences were amplified on cDNA obtained by reverse transcription of total RNA from 3rd instar larvae. PCR reaction using a high-fidelity DNA polymerase (Phusion, Biolabs) was performed with the following pair of primers, containing XbaI and BamHI restriction sites (underlined):
Forward 5'-ATATCTAGATCCGTAGTGCCACTGATGTTC-3';
Reverse 5'- TATGGATCCCTAGGCGGTGGAGGTCTCC-3'.
Amplified dCryAB PCR product was digested with BamH1 and Xba1 and cloned into pUASp-PL-Venus vector which was then injected into a w^{1118} embryos to produce transgenic flies, a step performed by the Fly Facility platform (www.fly-facility.com Clermont-Ferrand, France).
To introduce R120G and ABDmut point mutation into dCryAB we applied PCR-based mutagenesis. Two overlapping PCR products carrying point mutation were first generated with following pairs of primers (mutated nucleotides are underlined and in bold):
Forward 5'-ATATCTAGATCCGTAGTGCCACTGATGTTC-3'
Reverse R120Gmut 5'-AGCTGGTAGCGTC**C**GGAGAACTGGCGGG-3',
Reverse ABDmut 5'-GTCACATCGTCCCTCTCCTCC**T**ATGGCCTGCTGACCATCAAGGC-3'
Forward ABDmut 5'-GCCTTGATGGTCAGCAGGCCAT**A**GGAGGAGAGGGACGATGTGAC-3'
Forward R120Gmut 5'-CCCGCCAGTTCTC**C**GGACGCTACCAGCT-3'
Reverse 5'- TATGGATCCCTAGGCGGTGGAGGTCTCC-3',
2 µl of each PCR product carrying point mutation were mixed in 16 µl of water, heated to 99°C and annealed by cooling down to 37°C during 25 min. 2 µl of annealed PCR products were then used for final PCR amplification with Forward and Reverse primers. Cloning of mutated dCryABR120G and dCryAB ABDmut and generation of transgenics were as for the wild type UASp-Venus-dCryAB.

Mass spectrometry

We applied Mass Spectrometry (MS) to identify the dCryAB interacting proteins. Immunoprecipitation was performed as described below using dCryAB antibody on cytoplasmic protein extract from the dissected wild type larvae. The immunoprecipitated protein complexes were subjected to SDS-PAGE separation and Coomassie staining to

visualize bands of interest. Proteins ranging from 30 to 170 kDa were excised from the gel and analyzed by a specialized Mass Spectrometry and Proteomics Platform (MSPP, SupAgro INRA, Montpellier).

TEM

Dissected larvae (as described above) were fixed in 2,5% glutaraldehyde in 0,1M phosphate buffer, 3 times washed in phosphate buffer for 15 min, incubated over night and again washed 3 times. Material was post-fixated for 90min in the mixture of osmium tetroxide and potassium ferricyanide in the ratio 1:1. After dehydration in alcohol series (50%, 70%, 90%, 100%, 100%), material was embedded in a mixture acetone-epoxy resin in the ratio 1:1 and incubated for 24h in a very tight dish. The dish was opened for at least 7h for acetone to evaporate. Polymerization of material embedded in epoxy resin was performed during 24h at 45ºC and subsequently for 3 days at 60ºC. Ultrathin sections were observed in electron microscope Zeiss EM 900.

Immunogold

Dissected larvae (as described above) were fixed in 1:1 mixture of 0,5% glutaraldehyde and 4% paraformaldehyde in a PBS, at RT for 1,5h. Than the material was postfixed in 2% paraformaldehyde, at 4ºC overnight, washed in PBS with 0,5% TritonX100 (PBT) and dehydrated with graded ethanol series. After dehydration specimens were infiltrated in mixtures of 85% ethanol and LR White (London Resin Company Ltd) (2:1), (1:1), (1:2) 1h for each series. Then the material was infiltrated in two times with pure LR White for 12h at RT and once overnight at 4ºC and embedded in LR White and polymerized at 59ºC for 24h. Ultrathin sections were cut using an ultramicrotome (ReihertUltracut E). Ultrathin sections were preincubated for 2 h in 1% BSA in PBS. Then sections were incubated with primary antibodies: mouse anti-β-actin 1:10 and rat anti-dCryAB 1:500 at 4ºC overnight. After rinsing several times in PBT the material were incubated with secondary antibodies conjugated with gold particles. After washing in PBT, sections were contrasted with lead citrate for 2 min and analyzed using transmission electron microscope Zeiss EM 900.

Bioinformatics search for homologues

To compare amino acid sequences associated to dCryAB and CryAB, we used MUCLE (Multiple Sequence Comparison by Log-Expected) with default settings (McWilliam et al., 2013). We visualized the result with Jalview2 (Waterhouse et al., 2009) highlighting equivalences in red. Phylogenetic tree was built considering amino acid sequences of dCryAB, CryAB, Hspb1 and Hspb8 and those of some of their different homologues in various vertebrate and non-vertebrate species. We used phylogenetic analysis « One Click » pipeline available on (http://www.phylogeny.fr) to manage the different building steps and generate the final tree.

Supplemental figure legends

Figure S1. Double EM immunogold staining for dCryAB and actin showing that immunogold dots for dCryAB (18 nm of diameter) localize mainly to the Z-band but are also detected within the M-band. Note that small immunogold dots of 10 nm of diameter detecting actin are found at the Z-band. Scale bar 300 nm.

Figure S2. Effects of muscle targeted RNAi attenuation of dCryAB using VDRC 107305 line. (A) Lateral view of wild type dissected 3rd instar larval muscles from one hemisegment stained with phalloidin. Note altered pattern of sarcomeric actin suggesting disruption of Z-bands (arrowheads). (B) Statistical representation of muscle defects observed in examined *Mef>dCryAB-RNAi* larvae. (C) No significant changes in sarcomere size have been observed. (D) Significantly reduced number of sarcomeres observed in 3 different muscles (VL3, VL4 and SBM) in 3rd instar larvae with muscle-specific attenuation of dCryAB. (E-H) Affected contractility and muscle performance tests showing reduced motility of *Mef>dCryAB-RNAi* larvae. (I) No apoptotic events can be detected in *Mef>dCryABRNAi* muscles as judged by the activated Caspase 3 staining. Arrow points to cells that undergo apoptosis in the analyzed 3rd instar larvae preparation. Significant differences were determined by t-Student test. Asterisks indicate statistical level of significance of observed differences: *p<0,1, **p<0,5, ***p<0,001. Scale bar 40 μm.

Figure S3. Muscle targeted expression of dCryAB carrying mutated actin binding domain (ABD) affects sarcomeric actin pattern and nuclei positioning. The alignment of wild type and mutated amino acid sequence of dCryAB actin binding domain are shown. Mutated residue is in red and highly conserved residues are in bold (refer to Mounier and Arrigo, 2002). Arrows in (A) point to irregular actin pattern. Arrowheads in (A') indicated abnormally located dCryAB with mutated ABD whereas asterisk point to the area in which dCryAB-ABDmut displays a diffused pattern and is not detected in sarcomeres. Arrowheads in (A") denote clustered nuclei. Scale bar 50 μm.

Figure S4. Additional muscle defects observed after attenuation of *dCryAB*. (A) Muscle splitting (yellow arrowhead) with partial loss of splitted myofibrils. (B) Complete loss of a muscle. Arrowheads indicate position of extremities of lacking segment border muscle. Scale bar 40 μm. (C) Slightly but significantly reduced number of sarcomeres observed in 3

different muscles (VL3, VL4 and SBM) in 3rd instar larvae with muscle-specific attenuation of *dCryAB*. (D) No significant changes in sarcomere size have been observed. (E) *Mef>dCryAB-RNAi* animals display increased lethality at all developmental stages tested. Significant differences were determined by t-Student test. Asterisks indicate statistical level of significance of observed differences: *p<0,1, **p<0,5, ***p<0,001. Error bars indicate SEM.

Figure S5. dCryAB does not physically interact with Msp300. Western blot from IP experiment with anti-dCryAB on protein extract from 3rd instar larvae. Anti-Msp300 antibody was used to reveal immunoprecipitation reaction. Notice high molecular weight Msp-300 detected in the protein extract (Input) but not in the IP sample.

Figure S6. Bar graph representations of changes in heart parameters upon cardiac-restricted expression and knockdown of dCryAB. (A, B) Plot of mean systolic (A) and diastolic (B) intervals indicates shortening in contraction and relaxation phases for dCryAB lines. (C) Heart diastolic diameters for 1 week-old flies. Note the dilated diameters across the heart tube in $dCryAB^{R120G}$ flies. (D) Percent fractional shortening shows significant decrease when driving R120G dCryAB at 1 week old, in comparison to controls. Movies were taken from 20 flies for each genotype. Significant differences were determined by one-way ANOVA ([*] P<0.05; [**] P<0.005; [***] P<0.0005). Error bars indicate SEM.

Figure S7. Genetic interactions of dCryAB and cheerio and their impact on sarcomeric pattern. (A-A") Simultaneous RNAi knockdown of dCryAB and cheerio leads to misalignment of myofibrils (arrows in A) associated with severely affected sarcomeric actin and kettin patterns. High kettin level (asterisk in A') is detected in the sarcomeres displaying reduced/fuzzy actin (asterisk in A), a phenotype that has not been observed in muscles in which only dCryAB has been attenuated (see Fig. 4B). (B-B") Overexpression of dCryAB in cherRNAi context partially rescues irregular/fuzzy actin patterns observed in muscle with attenuated cheerio (Fig. 7E). Notice that some myofibrils misalignment can still be observed but sarcomeric kettin distribution appears regular in this context (B'). Scale bar 40 μm.

Figure S8. Muscle targeted RNAi knockdown of Starvin leads to misalignment of myofibrils and affected nuclei position but has no influence on sarcomeric and perinuclear localization of dCryAB. Arrows point to misaligned myofibrils and accumulation of dCryAB. Arrowheads indicate clustered nuclei. Scale bar 40 μm.

References:

Mounier N, Arrigo AP. Actin cytoskeleton and small heat shock proteins: how do they interact? Cell Stress Chaperones. 2002 Apr;7(2):167-76.

Table S1. Proteins identified by Co-IP with CryAB

Protein	**No. of matches/peptides**	**Protein**	**No. of matches/peptides**
Tropomyosin 1	108/19	α-actinin	18/12
Actin 57B	93/18	GlyP	18/10
Actin 87E	86/17	Ca-P60A	17/10
Actin 5C	66/16	PyK	16/12
Tropomyosin 2	61/11	Ef1 alpha 48D	16/7
Impl 3	47/15	Mp20	12/6
Arginine kinase	43/18	Pgi	11/6
Paramyosin	42/20	Pgm	10/8
Gapdh2	38/14	Hsp70	10/7
Gapdh1	33/11	Cheerio/dfilamin	9/6
MHC	25/19	Ef2b	8/6
Hsp60	24/13	Trip1	8/6

Supplementary figures

Figure S1

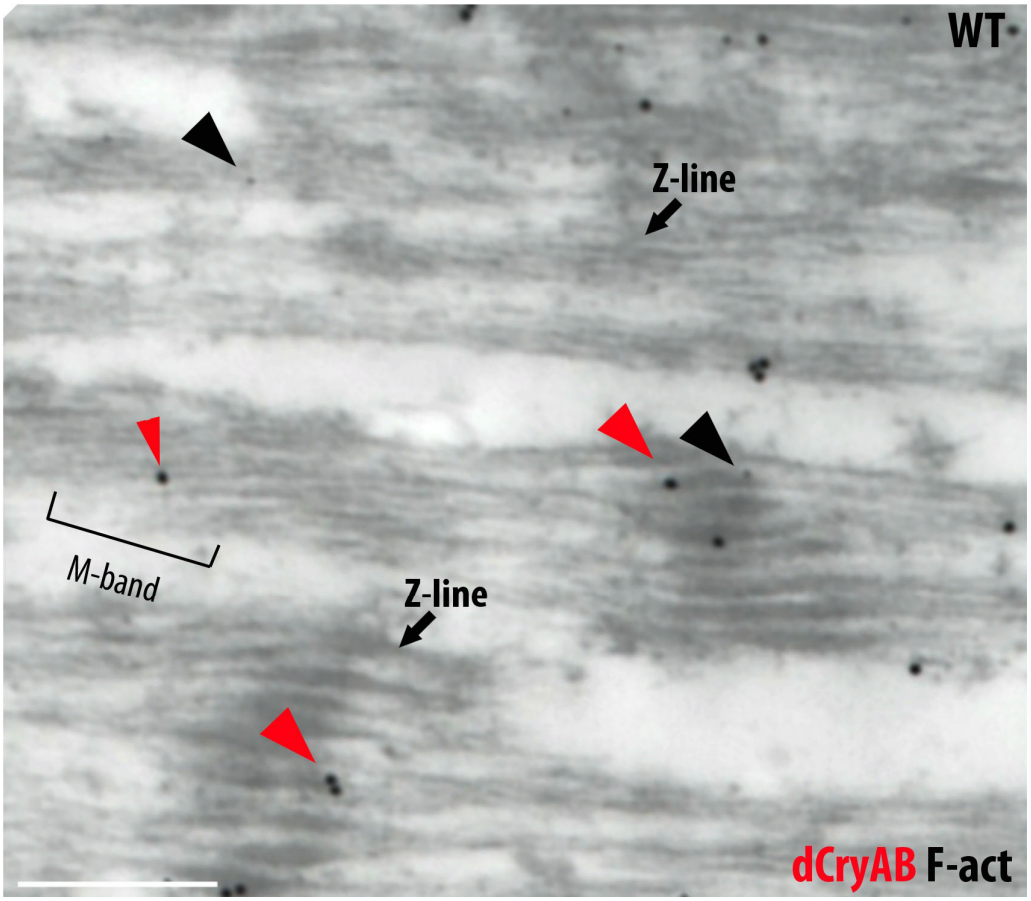

Figure S2

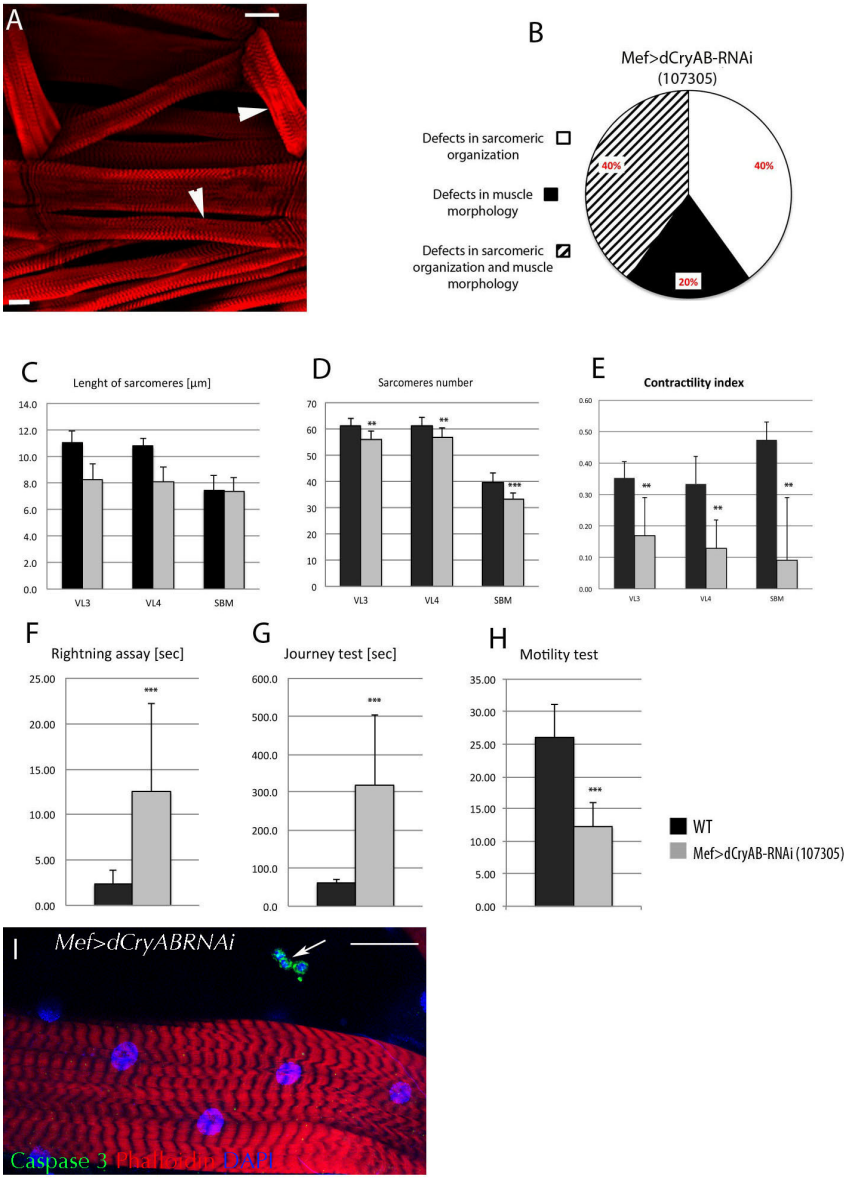
A
B
Mef>dCryAB-RNAi
(107305)
Defects in sarcomeric organization
Defects in muscle morphology
Defects in sarcomeric organization and muscle morphology
40%
40%
20%
C
Lenght of sarcomeres [µm]
VL3
VL4
SBM
D
Sarcomeres number
E
Contractility index
F
Rightning assay [sec]
G
Journey test [sec]
H
Motility test
WT
Mef>dCryAB-RNAi (107305)
I
Mef>dCryABRNAi
Caspase 3 Phalloidin DAPI

Figure S3

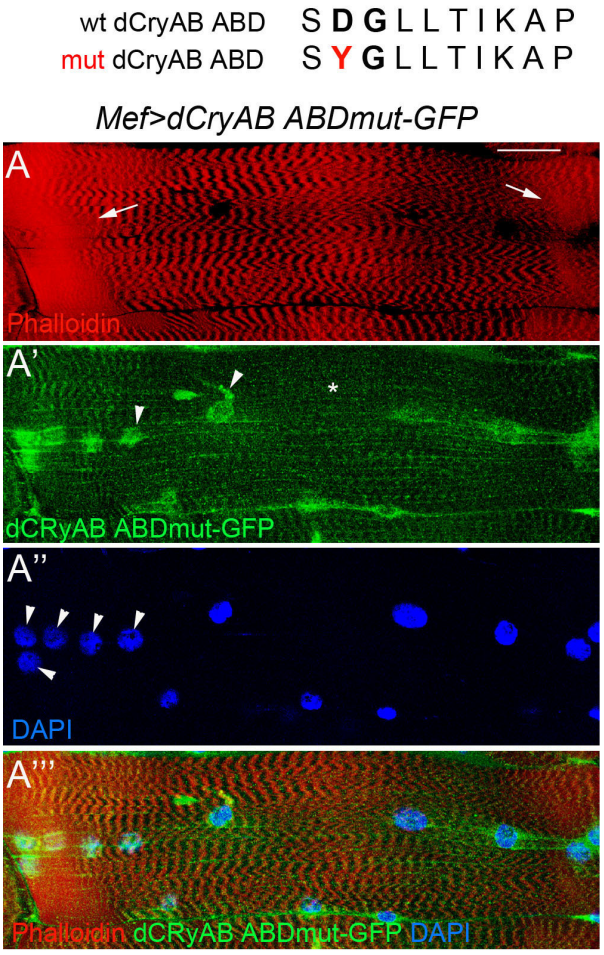
wt dCryAB ABD S D G L L T I K A P
mut dCryAB ABD S Y G L L T I K A P
Mef>dCryAB ABDmut-GFP
A
Phalloidin
A'
dCRyAB ABDmut-GFP
A''
DAPI
A'''
Phalloidin dCRyAB ABDmut-GFP DAPI

Figure S4

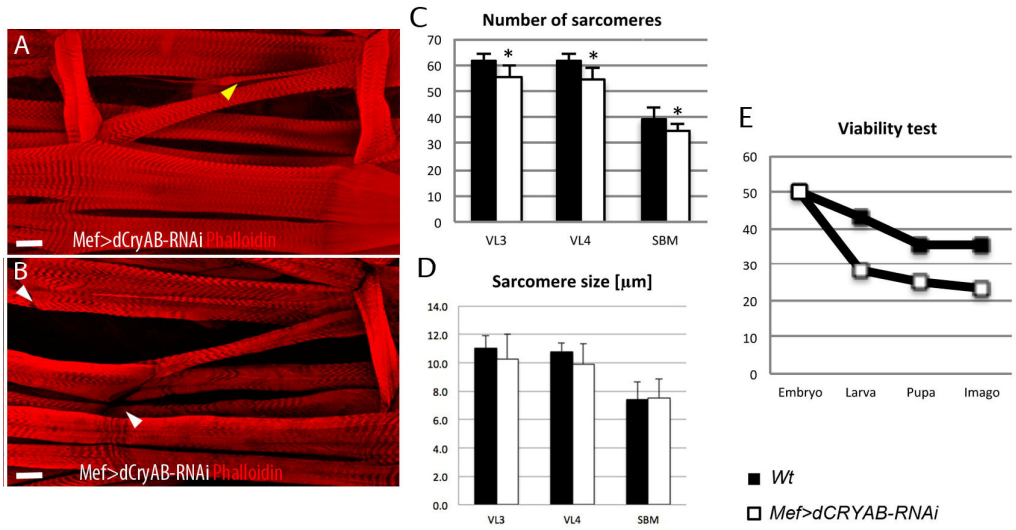

Figure S5

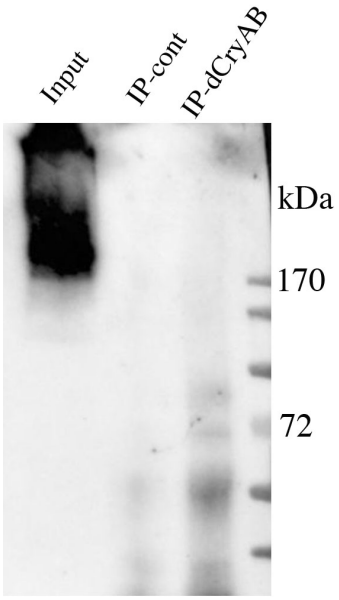

Figure S6

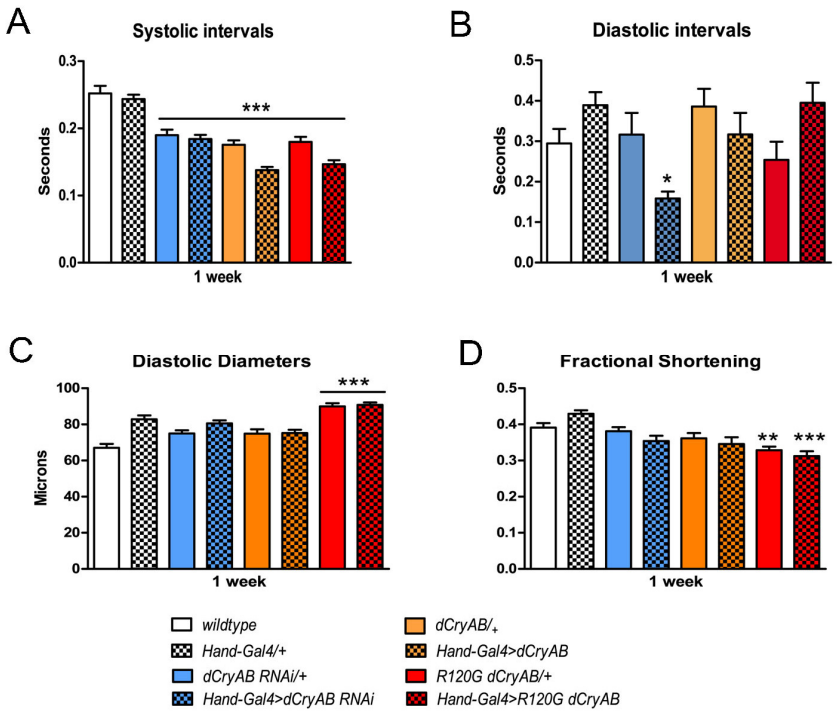

Figure S7

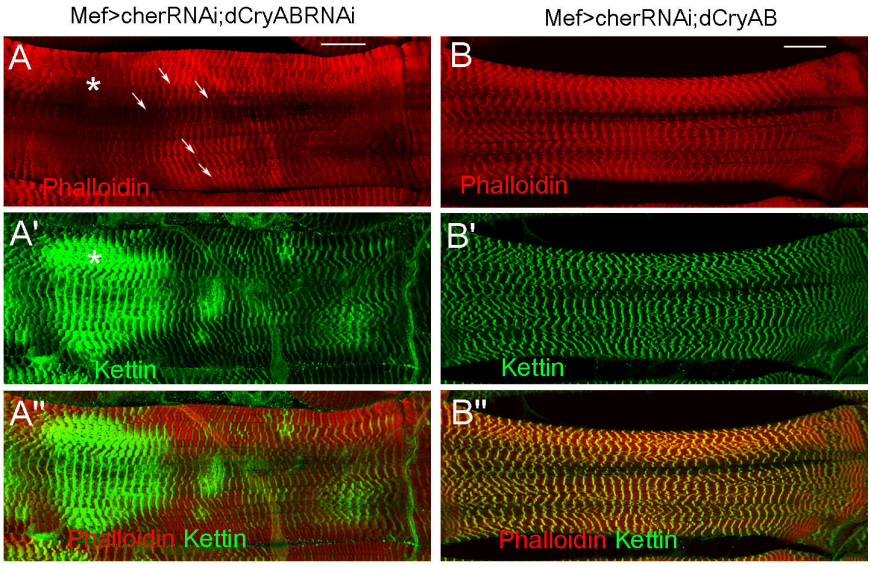

Figure S8

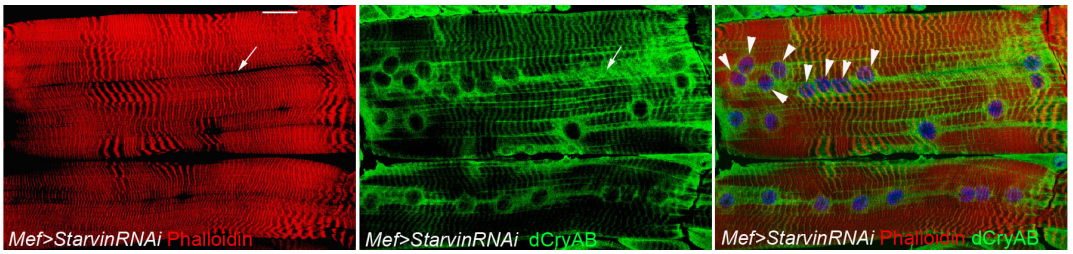
Mef>StarvinRNAi Phalloidin
Mef>StarvinRNAi dCryAB
Mef>StarvinRNAi Phalloidin dCryAB